2014

Examining physiological roles of adipose derived VEGF: Consequences in substrate availability and endurance exercise capacity in adipocyte specific VEGF deficient mice

Nicole J. Zachwieja
West Virginia University

Examining physiological roles of adipose derived VEGF: Consequences in substrate availability and endurance exercise capacity in adipocyte specific VEGF deficient mice

Nicole J. Zachwieja

Thesis submitted to the School of Medicine, Division of Exercise Physiology at West Virginia University in partial fulfillment of the requirements for the degree of Master of Science in Exercise Physiology

Committee:
I. Mark Olfert, Ph.D., Chair
Randall Bryner, Ed.D.
Linda Vona-Davis, Ph.D.

Division of Exercise Physiology

Morgantown, West Virginia
2014

Keywords: Vascular endothelial growth factor, adipose tissue, endurance exercise

ABSTRACT

Examining physiological roles of adipose derived VEGF: Consequences in substrate availability and endurance exercise capacity in adipocyte specific VEGF deficient mice

Nicole J. Zachwieja

Reducing vascular endothelial growth factor (VEGF) in adipose tissue alters adipose vascularity and metabolic homeostasis. We hypothesized that this would also affect metabolic responses during exercise-induced stress, and that adipocyte-specific VEGF deficient (adipoVEGF-/-) mice would have impaired endurance capacity. Endurance exercise capacity in adipoVEGF-/- (n=10) and littermate control (n=11) mice was evaluated every 4 weeks between 6 & 24 weeks of age using a submaximal endurance run to exhaustion at 20 m/min, 10-degree incline. Maximal running speed, using incremental increases in speed at 30-second intervals, was tested at 25 weeks of age. Beginning at 6 weeks, and continuing with all time points, endurance run time to exhaustion was 30% lower in adipoVEGF-/- compared to controls ($p<0.001$). The age-associated rate of decline in endurance capacity was similar in adipoVEGF-/- vs. control mice and there was no difference in maximal running speed between the groups. Following 1 hour of running at 50% maximum running speed, adipoVEGF-/- mice displayed decreased circulating insulin, ($p<0.001$), glycerol ($p<0.05$), and a tendency for decreased glucose ($p=0.06$) compared to controls. These data suggest that deficits in adipose tissue vasculature are mediated by adipose VEGF and that deficiency of VEGF blunts the availability of lipid-derived substrates during endurance exercise and affects insulin secretion and glucose metabolism.

TABLE OF CONTENTS

CHAPTER 1: INTRODUCTION

Vascular endothelial growth factor (VEGF) has been classically recognized as a potent, positive regulator of angiogenesis in both physiological and pathological contexts (Leung *et al.*, 1989). It has been suggested that VEGF action is dependent on the microenvironment, such that its activity and effects may be specific to the cell type from which it was produced (Olfert *et al.*, 2009, 2010). Recent studies have investigated the function of adipose-derived VEGF in regulating metabolic homeostasis through angiogenesis. Collectively, theses studies show that upregulation of VEGF in adipose tissue has beneficial metabolic effects, while deletion or inhibition of VEGF action (at the onset of diet induced obesity) has negative metabolic effects (Sun *et al.*, 2012; Elias *et al.*, 2012; Sung *et al.*, 2013).

Adipose-specific VEGF deficient (adipoVEGF-/-) mice on a high fat diet show decreased adipose capillarity, fat pad mass, body mass, and percentage body fat compared to controls (Sung *et al.*, 2013). This inability to deposit lipids in adipose tissue could also suggest a concurrent inability to sufficiently mobilize and utilize free fatty acids (FFA) as an energy substrate. Taken together, these observations suggest that alteration of VEGF can influence energy metabolism. This could be especially important, as VEGF has been reported to be altered with obesity, diabetes, and other chronic diseases (Wada *et al.*, 2011). At present, little is known about the role of adipose-derived VEGF in exercise capacity or metabolism in the context of exercise-induced stress.

Data from our laboratory has shown that adipoVEGF-/- mice exhibit decreased endurance capacity, but no difference in maximal running speed when compared to controls, suggesting a difference in use of lipid-derived substrates. CPT1 β is regarded as a rate-limiting enzyme of β-oxidation in skeletal muscle mitochondria (Schreurs *et al.*, 2010). Changes in CPT1β expression and β-oxidation could correlate with differences in endurance exercise

capacity, based on the amount of FFA made available to the muscles. Measurement of circulating lipid-derived energy substrates, as well as insulin and glucose in response to a submaximal bout of exercise can provide insight into how alterations in adipose tissue vasculature regulated by VEGF may influence exercise metabolism.

In the context of lipid-induced skeletal muscle damage, decreased β-oxidation leads to accumulation of lipids and hinders insulin signaling (Yu *et al.*, 2002). However, it is also argued that excessive β-oxidation due to increased intramuscular lipid content can overload mitochondrial capacity, leading to accumulation of metabolic intermediates and ultimately a decrease in mitochondrial function as well as interference with insulin signaling (Koves *et al.*, 2008).

Subsequently, it is unclear whether increased or decreased β-oxidation would be expected in adipoVEGF-/- mice. Blunted mobilization of FFA for use by working muscle may correlate with a decrease in β-oxidation and/or expression of CPT1β. However, adipoVEGF-/- mice exhibit increased lipid deposition in the liver, and lipid accumulation in the liver and skeletal muscles often coincide (Samuel *et al.*, 2010; Sung *et al.*, 2013). Measurement of intramuscular lipid content, along with mitochondrial protein expression of CPT1β can provide insight into whether skeletal muscle mitochondrial function may be affected by deficiencies in adipose tissue vasculature regulated by VEGF, ultimately contributing to deficits in endurance exercise capacity. Measurement of mitochondrial protein oxidation may provide indication of overloaded mitochondrial capacity leading to generation of reactive oxygen species. Overall, there is a need to determine how loss of VEGF in adipose tissue can result in decreased endurance capacity. This project has two specific aims to identify factors that may elicit such a response.

Specific Aim 1 is to determine whether decreased endurance exercise capacity in adipoVEGF-/- mice is associated with decreased FFA substrate availability during endurance exercise. It is hypothesized that adipoVEGF-/- mice will show decreased circulating FFA immediately following an exhaustive bout of endurance exercise, along with indications of greater reliance on glucose metabolism compared to littermate control mice.

Specific Aim 2 is to determine whether adipoVEGF-/- mice exhibit decreased endurance capacity due to dysfunction induced by lipid deposition in skeletal muscle. It is hypothesized that adipoVEGF-/- mice will show increased intramuscular triglycerides and subsequent skeletal muscle dysfunction when compared to controls.

Better understanding of the role of adipose VEGF in regulating exercise metabolism will broaden insights on the physiological function of VEGF. This knowledge will be important in developing effective therapeutic manipulations of the VEGF pathway in conjunction with exercise-based therapies.

CHAPTER 2: BACKGROUND AND SIGNIFICANCE

2.1 VEGF and VEGF Receptor Function

VEGF functions to promote angiogenesis and lymphangiogenesis by regulating the survival, proliferation and migration of endothelial cells. The VEGF family of proteins includes VEGF-A, VEGF-B, VEGF-C, VEGF-D, and VEGF-E. Placental growth factor (PlGF) is also included in this grouping and shows 42% homology of amino acids with VEGF-A (Maglione *et al.*, 1991; Byrne *et al.*, 2005). VEGF family signaling is conducted via binding to receptor tyrosine kinases, including VEGFR1 (Flt-1), VEGFR2 (Flk-1), and VEGFR3 (Flt-4). Each contains an extracellular domain, a transmembrane region, and a tyrosine kinase domain (Terman *et al.*, 1991). Upon binding of VEGF to its receptor, receptor molecules dimerize and tyrosine residues become phosphorylated and activated to elicit a downstream signaling response. VEGFR1 exists in both a membrane-bound and soluble form (sVEGFR1), which can each function to limit bioavailability of VEGF. Although VEGFR1 possesses an affinity for VEGF that is 10-fold greater than VEGFR2, the tyrosine kinase function of VEGFR1 is significantly less active than that of VEGFR2 (Park *et al.*, 1994). Therefore, it is thought that the membrane-bound isoform of VEGFR1 can also act as a negative regulator of VEGF function by limiting VEGF availability to the more active VEGFR2. Although cells that exclusively express VEGFR1 have been shown to participate in VEGF signaling responses, VEGFR2 is the primary mediator of VEGF signaling pathways in adult tissues (Gille *et al.*, 2001). VEGF receptors were originally identified on endothelial cells, but have since been identified on a nearly all cell types, including hematopoietic stem cells, vascular smooth muscle cells, tumor cells, and adipocytes (Byrne *et al.*, 2005).

VEGF-A (commonly, and hereafter referred to as VEGF) is thought to function mainly in angiogenesis. This VEGF gene possesses eight exons, producing seven different alternatively

spliced isoforms consisting of 121, 145, 148, 165, 183, 189, or 206 amino acids (termed $VEGF_{121}$, etc). Exons 1-5 are present across all isoforms, and all but $VEGF_{148}$ include exon 8 (Neufeld *et al.*, 1999). Alterative splicing occurs at exons 6 and 7, which code for two heparin-binding domains. The presence/absence of exons 6 and 7 determine how diffusible or how tightly bound each isoform is to the cell surface. Isoforms possessing both exons 6 and 7 have the greatest affinity for the cell surface. The most prevalent isoform and strongest stimulator of angiogenesis is $VEGF_{165}$. This isoform lacks only exon 6, is somewhat diffusible, and is capable of binding both the extracellular matrix and heparin (Park *et al.*, 1993). The VEGF protein is a 42 kDa, dimeric glycoprotein playing a key role in angiogenesis-mediated physiological functions such as embryogenesis, wound healing, and the reproductive cycle. Non-malignant disease related functions of VEGF are involved in rheumatoid arthritis, diabetes, ischemic retinopathies, and other conditions. VEGF also plays a large role in supporting tumor development by stimulating growth of vasculature to support malignant cells (Hoeben *et al.*, 2004).

The activation and downstream effects of VEGF involve many cellular pathways. Two important molecules associated with well-characterized VEGF pathways include hypoxia inducible factor-1 (HIF-1), which plays an upstream role in VEGF activation, and nitric oxide (NO), a downstream target of VEGF signaling. Tissue oxygen supply is an important regulator of VEGF expression. The HIF-1 protein complex, consisting of HIF-1 α and HIF-1β subunits, binds to the VEGF gene's enhancer sequence. Under conditions of appropriate oxygen supply, HIF-1 α is degraded. However, under hypoxic conditions, this degradation is inhibited and the HIF-1 complex is able to bind the VEGF enhancer sequence. This allows for upregulation of VEGF, and in theory, stimulated vessel growth to facilitate increased oxygen delivery to the

tissue (Iyer *et al.*, 1998). VEGF binding to VEGFR2 initiates a signaling cascade activating phosphatidylinositol 3'-kinase (PI3K), which in turn activates endothelial nitric oxide synthase (eNOS), generating NO. NO is a potent vasodilator and also allows for increased permeability of the vasculature, cellular migration, and exerts overall pro-angiogenic effects (Fulton *et al.*, 1999; Cooke, 2002).

2.2 Adipose-specific VEGF

Interestingly, a role for VEGF in metabolism has recently been identified. In an investigation of specific effects of VEGF in skeletal muscle, microarray analysis in muscle-specific VEGF deficient mice showed differential expression (compared with littermate controls) of several genes involved in lipid metabolism and metabolic disease (Olenich SA, Audet GN, Szeszel-Federowicz V, Chen D, 2012). Additionally, reduced capillarity in skeletal muscles of muscle-specific VEGF deficient mice leads to increased insulin resistance and maladaptation to exercise training (Olfert *et al.*, 2010; Bonner *et al.*, 2013; Gorman *et al.*, 2014).

Adipose tissue is highly vascularized, and capillaries within the tissue function to deliver oxygen, nutrients, growth factors, cytokines, stem cells, monocytes and neutrophils via the blood supply. This vasculature also functions to remove waste products from the tissue and to mobilize fatty acids to be used as energy substrates. In addition, it has been shown that endothelial cells produce growth factors and cytokines that interact with adipocytes, and vascular pericytes can differentiate into preadipoctyes and adipocytes (Cao, 2010). Thus, the vasculature is an important component of adipose development, health, and plasticity, which greatly affects overall metabolic health.

It follows that studies have investigated the specific role of adipocyte-derived VEGF in the context of metabolic dysfunction. Elias et al. (2012) found that mice overexpressing VEGF

in adipose tissue were protected against hypoxia and obesity in response to high fat feeding. Obesity is described as an excess of adipose tissue in the body (Yach *et al.*, 2006). With the ability of adipose tissue to grow and expand continuously, chronic exposure to a high fat diet delivers a constant supply of triglycerides to this tissue, leading to obesity in most cases (Cao, 2010). In mice, diets containing approximately 40-60% kilocalories (kcal) from fat are commonly used to induce obesity, and consequently metabolic dysfunction (Surwit *et al.*, 1988; Sung *et al.*, 2013). Adipose tissue functions as an endocrine organ, secreting adipokines (growth factors and cytokines produced by adipocytes) that participate in both local and systemic modifications (Waki & Tontonoz, 2007). Excess adipose tissue is associated with increased expression of proinflammatory factors, as well as circulating FFA, which can each contribute to metabolic disease (Björntorp *et al.*, 1969; Weisberg *et al.*, 2003). It has been proposed that the cause of this inflammatory response in obesity has links to oxidative stress and hypoxia (Sung *et al.*, 2013).

The protection from diet-induced (42% kcal from fat) obesity and hypoxia as a result of increased adipose VEGF shown by Elias et al. (2012) was associated with improvements in insulin sensitivity and glucose tolerance. Infiltration of anti-inflammatory macrophages into adipose tissue was also observed, as well as increased thermogenesis and energy expenditure (Elias *et al.*, 2012). Sun et al. (2012) reported similar findings in mice overexpressing adipose VEGF, including transition of white adipose tissue to a more metabolically active "brown-like adipose tissue" phenotype through the potent, local upregulation of PGC1α and UCP1. Stimulation of VEGF expression had overall positive metabolic effects when induced at the onset of diet-induced (60% kcal from fat) weight gain, while interfering with VEGFR2 action

also showed positive effects, such as improved insulin resistance, in the context of pre-existing obesity using an *ob/ob* mouse model (Sun *et al.*, 2012).

2.3 Adipose-specific VEGF Deficient Mice

Sung et al. (2013) have recently characterized an adipoVEGF-/- mouse model. This Cre-LoxP transgenic approach used the fatty acid binding protein 4 (fabp4, also known as ap2) promoter to limit the transcription of Cre recombinase (Cre) to the adipocyte, where it excises the DNA sequence between LoxP sites surrounding the exon 3 coding region of the VEGF gene (Gerber *et al.*, 1999; Nagy, 2000; He *et al.*, 2003). This region is required for VEGF to bind to its receptors. In the presence of Cre expression, this region is excised and VEGF becomes inactive in adipose tissue.

In this model, adipoVEGF-/- mice under basal diet conditions showed little to no mRNA and protein expression of adipocyte VEGF with no change in circulating VEGF levels, a 50% decline in capillarity in white and brown adipose tissue, and decreases in body mass, percentage body fat, and fat pad mass. Expression of VEGFR2 was also decreased, along with decreased adiponectin and increased TNF α mRNA expression. These mice displayed diminished ability to appropriately handle oral lipid challenge by showing greatly increased circulating FFAs 3 hours following an oil gavage (Sung *et al.*, 2013). In response to a high fat diet challenge (60% kcal from fat), both body and fat pad mass were decreased and insulin resistance was observed. Importantly, circulating FFAs were decreased and liver triglycerides were increased. Lipid droplets were observed in the liver around portal veins in adipoVEGF-/- mice but not in controls (Sung *et al.*, 2013). Insulin resistance has been associated with deposition of lipids in both liver (steatosis) and skeletal muscle, and coincident lipid accumulation in these tissues has been used as a determinant for insulin resistance in obese humans (Samuel *et al.*, 2010). Thus, although

increased intramuscular triglycerides were not specifically shown in the characterization of the adipoVEGF-/- mouse, lipid accumulation in the liver and skeletal muscles often coincide and result in increased morbidity. Additionally, Sung et al. (2013) observed inflammation and metabolic dysfunction resulting from hypoxia and adipocyte apoptosis in response to high fat diet in adipoVEGF-/- mice. This group proposed that hypoxia in adipose tissue (due to lack of VEGF-mediated vascular growth) triggers a series of events including adipocyte apoptosis, followed by inflammation, ectopic lipid deposition, and lipotoxicity, which culminates in insulin resistance.

2.4 Adipose VEGF and Exercise

Although an expanding body of work describes the effects of both gain and loss of adipose-specific VEGF function in the context of metabolic syndrome, much less is known about the role of adipose VEGF in the metabolic challenges triggered by exercise. *Muscle*-specific VEGF deficient mice have been characterized and show decreased endurance capacity and an inability to exhibit vascular adaptations to training, indicating an important role for myocyte-derived VEGF in exercise adaptation (Olfert *et al.*, 2009, 2010). This provides additional evidence for tissue-specific roles of VEGF in exercise. A small number of studies have shown an association between exercise training and an increase in VEGF mRNA in adipose tissue of mice and rats (Hatano *et al.*, 2011; Baynard *et al.*, 2012). Czarkowska-Paczek et al. (2011) described a similar increase in adipose VEGF mRNA following exercise training, but at the same time reported that VEGF protein levels remained unchanged. Therefore, there is a need to better characterize the association between exercise and adipocyte VEGF protein expression. There is a need to better understand the effects of adipose-derived VEGF on exercise capacity, the

mechanisms by which observed changes might be regulated, and overall metabolic effects that may be mediated by adipose VEGF in the context of exercise-induced stress.

2.5 Exercise Metabolism

The utilization of substrates to provide working tissues with energy has been extensively studied and characterized under varying intensities and types of exercise. In general, very short duration exercise (i.e. up to 20 seconds) at a high intensity uses primarily creatine phosphate, which donates a phosphate group to ADP to form ATP for energy. However, high intensity exercise exceeding approximately five seconds begins to require the input from anaerobic glycolysis, and reliance on this pathway increases with up to around 45 seconds of high intensity exertion. At this point, contribution from aerobic energy production systems begins to take effect. By two minutes of exertion, anaerobic and aerobic pathways make an equal contribution (Hultman, 1973). Prolonged bouts of exercise primarily require energy from aerobic metabolism. Both lipids and carbohydrates (and less frequently, proteins) can be used as energy-producing substrates in aerobic metabolism. Exercise intensity governs the type of fuel to be oxidized, such that increasing intensity elicits greater reliance on carbohydrate metabolism. At rest, fat metabolism is the primary contributor to energy production, and this steadily decreases as exercise intensity increases. The "crossover concept" describes this shift from reliance on fat to carbohydrate metabolism with increasing exercise intensity. Thus, fat is a significant fuel source for prolonged low-intensity exertion, and fat oxidation progressively increases with time during such a bout of exercise (Powers & Howley, 2007). As a critical regulator of adipose tissue vasculature, adipocyte VEGF can in turn affect the ability for this critical energy substrate to be mobilized and oxidized during sustained submaximal exercise (Powers & Howley, 2007).

Epinephrine, norepinephrine and glucagon stimulate action of lipases, which break down FFAs from triglycerides in adipose tissue stores, releasing them into the bloodstream to be delivered to the working tissue. Other positive regulators of lipolysis include growth hormone, cortisol, thyroid hormones, and leptin (Horowitz, 2003). Insulin acts as an inhibitor of this process (Pascual *et al.*, 1995). Fatty acid binding protein, fatty acid transport protein and fatty acid translocase (CD36) all function to move FFAs into the muscle cell (Bonen *et al.*, 2000). Intramuscular triglycerides also serve as a site of storage for lipid to be used as fuel. Once a long-chain fatty acid is inside the cell, it can be activated by an acyl-CoA synthase, creating a long-chain fatty acyl-CoA. Carnitine palmitoyltransferase 1 (CPT1β, the muscle isoform) moves the acyl-CoA across the outer mitochondrial membrane, exchanging the CoA group for carnitine to form a long-chain acylcarnitine. Carnitine acylcarnitine translocase transports this molecule across the inner mitochondrial membrane and Carnitine palmitoyltransferase 2 (CPT2) exchanges the carnitine group for a CoA, again creating a long-chain fatty acyl-CoA. Now in the mitochondrial matrix, this fatty acyl-CoA undergoes β–oxidation, a series of steps that cleave 2 carbon fragments off the fatty acid chain, forming molecules of acetyl-CoA, which can then enter the Krebs cycle and be used for oxidative metabolism and ATP production (Schreurs *et al.*, 2010). Therefore, CPT1β is considered to be a rate-limiting enzyme of the β-oxidation process in skeletal muscle.

The respiratory exchange ratio (RER, also known as RQ) is used to indicate the type of fuel being used by the body. RER is calculated as volume of carbon dioxide produced divided by the volume of oxygen consumed by an individual. Under steady state conditions (for example, when the subject is not engaging in hyperventilation), RER is an appropriate estimation of RQ. The oxidation of one fatty acid chain produces a ratio of carbon dioxide to oxygen that is

equal to 0.7, while the oxidation of glucose produces a ratio equal to 1.0. An RER of 0.7 is said to indicate that one is using fat as the primary fuel source, while an RER of 1.0 indicates primary reliance on carbohydrates. However, it is most realistic that a combination of fat, carbohydrate, and (to a small degree) protein metabolism is used during submaximal exercise. RER values between 0.7 and 1.0 are common, in which increasing RER indicates increasing reliance on carbohydrate metabolism (Powers & Howley, 2007).

2.6 Lipid-Induced Skeletal Muscle Dysfunction

Adipocyte VEGF can potentially influence fatty acid mobilization, an important factor allowing use of lipid-derived energy to sustain prolonged low-intensity exercise. However, another important scenario to consider in the context of adipose VEGF deficiency is ectopic lipid deposition and the promotion of insulin resistance and mitochondrial damage. With the inability to be appropriately deposited in adipose tissue, lipids tend to accumulate in the liver, and likely in other organs such as skeletal muscle (Sung *et al.*, 2013).

There are two proposed mechanisms for the cause of lipid-induced insulin resistance in skeletal muscle. First, it is argued that decreased β–oxidation and thus accumulation of lipids leads to serine phosphorylation of insulin receptor substrate 1 (IRS-1), hindering insulin signaling (Yu *et al.*, 2002). Second, other accounts provide evidence that excessive β–oxidation overloads mitochondrial metabolic capacity and leads to incomplete fatty acid oxidation and an accumulation of metabolic intermediates can lead to mitochondrial stress, insulin resistance, and overall decreases in function (Koves *et al.*, 2008). Generation of reactive oxygen species (generally produced by high levels of metabolic processes) has been shown to activate serine kinases that phosphorylate IRS-1, a possible mechanism by which excessive β–oxidation could contribute to insulin resistance (Bloch-Damti & Bashan, 2005). Detrimental effects of

incomplete fatty acid oxidation are further supported by the "athlete's paradox." Goodpaster et al. (2001) provide evidence that obese, sedentary individuals display insulin resistance due to elevated intramuscular lipid content, while lean athletes show similarly elevated intramuscular triglycerides but are able to appropriately use them as a fuel source due to high oxidative capacity, and therefore do not experience the same negative effects. Additionally, links have been shown between oxidative stress, compromised mitochondrial respiration and decreased exercise capacity in diabetic mice (Yokota *et al.*, 2009). Collectively, these findings provide evidence that increased lipid content and insufficient oxidative capacity in skeletal muscle can contribute to decreased exercise capacity due to insulin resistance and mitochondrial damage.

2.7 Links between Adiposity, Age, Sex, and Exercise

Sex differences exist in body fat distribution such that female mammals possess relatively more subcutaneous and fat in the lower-body region, while males tend to deposit more visceral fat, which is associated with increased risk of heart disease and type 2 diabetes (Chen *et al.*, 2012). Studies point to estrogens, progestins, and androgens as contributors to these differences. Menopause-related decreases in these hormones in women are associated with increased adipose tissue accumulation in the abdominal region (Brown *et al.*, 2010). Interestingly, subcutaneous fat is considered to be a greater contributor of FFA delivery to skeletal muscle for energy use during exercise (Horowitz, 2003).

During the aging process, general decreases in bone mineral density and skeletal muscle mass occur, along with increased accumulation of adipose tissue (Fontana & Klein, 2007). It has been shown in humans and rodents that mutations to mitochondrial DNA occur naturally with age. This leads to systemic degeneration and decreased stress tolerance, contributing to decreased exercise capacity (Khaidakov *et al.*, 2003). However, mice engaging in regular

endurance exercise throughout their life span are shown to be protected from age-related mitochondrial dysfunction (Safdar *et al.*, 2011).

2.8 Summary of Background and Significance

VEGF is an important stimulator of tissue angiogenesis, and has been shown to be important in the metabolic function of adipose tissue. Loss of adipose VEGF results in detrimental metabolic effects and decreased endurance exercise capacity in mice, however little is known about the direct role of adipose VEGF in this context. VEGF deficiency in adipose tissue can potentially lead to decreased ability to mobilize and utilize FFA, an important fuel source during sustained submaximal exercise. Additionally, inability to deposit FFA in adipose stores leads to ectopic lipid deposition. In skeletal muscle, increased lipid deposition in the absence of compensatory increases in oxidative capacity leads to mitochondrial damage and insulin resistance. Consequently, there is a need to clarify the role for adipocyte VEGF in influencing factors that can contribute to exercise intolerance.

CHAPTER 3: MANUSCRIPT

Adipocyte specific VEGF deficient mice show altered substrate availability and diminished endurance exercise capacity

Nicole J. Zachwieja[1], Grant C. O'Connell[1], Janelle C. Stricker[1], Jessica Allen[5], Linda Vona-Davis[2,4] and I. Mark Olfert[1,3,4]

West Virginia University School of Medicine, One Medical Center Dr., Morgantown, WV 26506
(1) Division of Exercise Physiology
(2) Department of Surgery
(3) Center for Cardiovascular and Respiratory Sciences
(4) Mary Babb Randolph Cancer Center
(5) Concord University, 1000 Vermillion St., Athens, WV 24712

Short Title: Adipose VEGF and endurance exercise
Total words: TBD

Corresponding Author:
Mark Olfert, Ph.D.
West Virginia University School of Medicine
Center for Cardiovascular and Respiratory Sciences
Division of Exercise Physiology
One Medical Center Dr.
Morgantown, WV 26506-9105
Tel 304-293-7597
Fax 304-293-5513
molfert@hsc.wvu.edu

ABSTRACT

Reducing vascular endothelial growth factor (VEGF) in adipose tissue alters adipose vascularity and metabolic homeostasis. We hypothesized that this would also affect metabolic responses during exercise-induced stress, and that adipocyte-specific VEGF deficient (adipoVEGF-/-) mice would have impaired endurance capacity. Endurance exercise capacity in adipoVEGF-/- (n=10) and littermate control (n=11) mice was evaluated every 4 weeks between 6 & 24 weeks of age using a submaximal endurance run to exhaustion at 20 m/min, 10-degree incline. Maximal running speed, using incremental increases in speed at 30-second intervals, was tested at 25 weeks of age. Beginning at 6 weeks, and continuing with all time points, endurance run time to exhaustion was 30% lower in adipoVEGF-/- compared to controls ($p<0.001$). The age-associated rate of decline in endurance capacity was similar in adipoVEGF-/- vs. control mice and there was no difference in maximal running speed between the groups. Following 1 hour of running at 50% maximum running speed, adipoVEGF-/- mice displayed decreased circulating insulin, ($p<0.001$), glycerol ($p<0.05$), and a tendency for decreased glucose ($p=0.06$) compared to controls. These data suggest that deficits in adipose tissue vasculature are mediated by adipose VEGF and that deficiency of VEGF blunts the availability of lipid-derived substrates during endurance exercise and affects insulin secretion and glucose metabolism.

Abbreviations

adipoVEGF-/-, adipose specific VEGF deficient; BAT, brown adipose tissue; C:A, capillary to adipocyte ratio; C:F, capillary to muscle fiber ratio; CPT1β, carnitine palmitoyltransferase-I beta; Cre, cre recombinase; Fabp4, fatty acid binding protein 4; FFA, free fatty acids; PGC1α, peroxisome proliferator-activated receptor gamma coactivator 1-alpha; PLT, plantaris muscle;

SOL, soleus muscle; UCP1, uncoupling protein 1; VEGF, vascular endothelial growth factor; WAT, white adipose tissue

INTRODUCTION

Vascular endothelial growth factor (VEGF) has been classically recognized as a potent, positive regulator of angiogenesis in both physiological and pathological contexts (Leung *et al.*, 1989). It has been suggested that VEGF action is dependent on the microenvironment, such that its activity and effects may be specific to the cell type from which it was produced (Olfert *et al.*, 2009, 2010). Recent studies have investigated the function of adipose-derived VEGF in regulating metabolic homeostasis through angiogenesis (Sun *et al.*, 2012; Elias *et al.*, 2012; Sung *et al.*, 2013).

Adipose tissue is highly vascularized, and capillaries that surround adipocytes function to deliver oxygen, nutrients, growth factors, cytokines, stem cells, monocytes and neutrophils via the blood supply. This vasculature also functions to remove waste products from the tissue and to mobilize fatty acids to be used as energy substrates (Cao, 2010). Thus, the vasculature is an important component of adipose development, health, and plasticity, which greatly affect overall metabolic health. Studies have investigated the specific role of adipocyte-derived VEGF in the context of metabolic dysfunction (Sun *et al.*, 2012; Elias *et al.*, 2012; Sung *et al.*, 2013). For example, Elias *et al*. (2012) found that mice overexpressing VEGF in adipose tissue were protected against hypoxia and obesity in response to high fat feeding, along with displays of increased insulin sensitivity and glucose tolerance. Sun *et al.* (2012) have reported similar findings in mice overexpressing adipose VEGF, including transition of white adipose tissue to a more metabolically active "brown-like adipose tissue" phenotype through the potent, local upregulation of peroxisome proliferator-activated receptor gamma coactivator 1-alpha (PGC1α)

and uncoupling protein 1 (UCP1). Finally, Sung *et al.* (2013) have recently show that adipose-specific VEGF deficient (adipoVEGF-/-) mice on a high fat diet show decreased adipose capillarity, fat pad mass, body mass, and percentage body fat compared to controls. AdipoVEGF-/- mice also exhibit increased lipid deposition in the liver. Lipid accumulation in the liver and skeletal muscles often coincide, and increased fat deposition in skeletal muscle has been shown to induce mitochondrial dysfunction (Koves *et al.*, 2008; Samuel *et al.*, 2010). This inability to deposit lipids in adipose tissue could also suggest a concurrent inability to sufficiently mobilize and utilize free fatty acids (FFA) as an energy substrate. Taken together, these observations suggest an important link between adipose VEGF and alteration of energy metabolism. While a small number of studies have shown an association between exercise and an increase in VEGF mRNA in adipose tissue of mice and rats (Hatano *et al.*, 2011; Baynard *et al.*, 2012), little is known about the role of adipose-derived VEGF in exercise capacity and exercise metabolism.

The purpose of this study was to evaluate endurance capacity and substrate utilization in response to exercise in adipoVEGF-/- mice compared to controls. We hypothesize that adipoVEGF-/- mice will show decreased endurance running capacity compared to controls, owing to an inability to mobilize and utilize lipid-derived energy from adipose tissue stores during submaximal exercise. To test this hypothesis, we performed submaximal endurance and maximal running speed testing at several time points in adipoVEGF-/- and control mice, and subsequently measured levels of circulating glucose, insulin, glycerol and free fatty acids (FFA) in response to a one-hour submaximal run. We also examined protein expression of carnitine palmitoyltransferase-I β (CPT1β) in mitochondria isolated from skeletal muscle of these mice to

investigate potential differences in β-oxidation, as well as mitochondrial protein oxidation to gauge mitochondrial health.

MATERIALS AND METHODS

All experiments were approved by and conducted in accordance with the guidelines of the West Virginia University Institutional Animal Care and Use Committee. All mice were kept on a 12-hr light/dark cycle schedule, housed between 2 and 5 to a cage and given access to a standard chow diet and water *ad libitum,* except when otherwise noted.

Generation of adipoVEGF-/- mice: Mice expressing Cre recombinase (Cre) under control of the fatty acid binding protein 4 (fabp4) promoter were purchased from The Jackson Laboratory (stock no. 005069, Bar Harbor, ME). This line was crossed with a VEGF LoxP line originally obtained from Dr. Napoleone Ferrarra (Gerber *et al.*, 1999) to produce a line in which VEGF expression is "knocked down" in white and brown adipose tissue (adipoVEGF-/-). Both lines are of the C57BL/6 background. All experimental animals were homozygous for the presence of LoxP sites on the VEGF gene. AdipoVEGF-/- mice possessed the fabp4/Cre transgene (Cre+), while littermate control mice did not express the Cre gene (Cre-) (Figures 1A and 1B).

Genotyping was carried out via 2 separate PCR reactions performed on genomic DNA extracted from tail snips of weanlings using an all-in-one tail lysis buffer (Allele Biotechnology). For detection of VEGF LoxP sites, forward primer 5'-TCCGTACGACGCATTTCTAG-3' and reverse primer 5'-CCTGGCCCTCAAGTACACCTT-3' were used. VEGF LoxP PCR products were amplified using 30 cycles of 94°C for 1:15, 53°C for 1:39, and 72°C for 2:50. For detection of Cre, forward primer 5'-GCATTACCGGTCGATGCAACGAGTG-3' and reverse primer 5'-GAACGCTAGAGCCTGTTTTGCACGTTC-3' were used. An internal control

primer set of forward 5'-ACGTACATGGCTGGGGTGTT-3' and reverse 5'-ACAGTTTCACCTGCCCTGAGT-3' were also used in this reaction. Cre PCR products were amplified using 35 cycles of 94°C for 0:20, 59°C for 0:30, and 72°C for 0:55 and all products were resolved and visualized using gel electrophoresis.

VEGF Expression in adipoVEGF-/- Tissues: To show instance of deletion between LoxP sites within the VEGF gene, genomic DNA was isolated from white adipose tissue (WAT), brown adipose tissue (BAT) and gastrocnemius skeletal muscle using a DNeasy Blood and Tissue Kit (Qiagen, Valencia, CA) according to the manufacturer's instructions (n=4 male adipoVEGF-/- and 4 male control samples per tissue type). Primer binding sites were situated outside of the LoxP sites, such that a PCR product could only be formed if the region between LoxP sites had been excised by Cre (the alternative product is too large to be amplified). For detection of deletion, forward primer 5'-CTTCATGGACAGGCTTCGGT-3' and reverse primer 5'-GCCCATATTCCAGAGACGGG-3' were used. PCR products were amplified using 30 cycles of 94°C for 0:30, 55°C for 0:45, and 72°C for 1min. Products were resolved using gel electrophoresis (ethidium bromide-stained agarose gel, 1.5%) and imaged using Genesnap software (version 7.01) from a digital imager (G-Box Chemi16, Syngene, Cambridge, UK). To analyze VEGF mRNA expression, total RNA was extracted from WAT, BAT and GA using an RNeasy Lipid Tissue Mini Kit (Qiagen, Valencia, CA) according to the manufacturer's instructions (n=4 male adipoVEGF-/- and 4 male control samples per tissue type). Reverse transcription was performed using a High Capacity cDNA Reverse Transcription Kit (Applied Biosystems, Foster City, CA). For detection of VEGF, forward primer 5'-GGCCTCCGAAACCATGAACT-3' and reverse primer 5'-AGCTTCGCTGGTAGACATCC-3' were used. For an internal loading control, QuantumRNA™ 18S Internal Standards primers

(Ambion®, Austin, TX) were used according to the manufacturer's instructions. PCR products were amplified, resolved and imaged as described above. Relative VEGF expression was determined by normalizing the optical density of the VEGF product band to that of the 18s product band using NIH ImageJ software (version 1.46r).

Exercise Protocols and Body Composition Analysis: For all experiments, adipoVEGF-/- mice (n=10; 5 males, 5 females) mice and littermate controls (n=11; 7 males, 4 females) were used. Mice were subjected to sub-maximal endurance exercise testing once every 4 weeks, starting at 6 weeks and continuing to 24 weeks of age. The running speed used for sub-maximal endurance testing was determined based on a targeted range of percentage of maximal running speed correlating with a range of exercise intensity that would elicit reliance on fat metabolism. Running speed has been shown correlate closely with oxygen uptake in untrained mice and rats. Maximal treadmill running speed ranges between 35 and 45 m/min in untrained C57BL/6 mice (Høydal *et al.*, 2007; Olfert *et al.*, 2009; Malek & Olfert, 2009). Based on this range, it was determined that submaximal endurance testing conducted at 20 m/min would elicit between 44% and 57% effort (with % effort increasing to the higher end of this range with increasing age). Mice were placed on a treadmill (Columbus Instruments, Exer-6M Treadmill, Columbus, OH) set at a 10° incline and were given a few minutes to acclimate to the new environment. A warm-up period was then allowed, consisting of running for 5 min at 4 m/min, 2 min at 10 m/min and 2 min at 15 m/min. The speed was then increased to 20 m/min and kept constant until the animal was unable to continue, and total time to exhaustion was recorded. Exhaustion was defined as the point at which the animal could no longer get back on to the treadmill and continue running, despite receiving electric shock from the grid located just underneath the end of the treadmill belt. At 25 and 37 weeks of age, each animal completed a maximal running capacity test. This

test consisted of running at a 10° incline, beginning with a 5 min warm-up period at 4 m/min and then increasing speed in increments of 2 m/min every 30 sec until exhaustion. Maximum running speed achieved was recorded. Body composition analysis was conducted on each animal 24 hours prior to the endurance run test at each time point using an EchoMRI-100 analyzer (Houston, TX), which gave *in vivo* measurements (in grams) of total body fat mass and lean mass.

Oral Glucose Tolerance Test: All blood glucose measurements (TRUEtest, Walgreen Co.) were conducted using a small sample of tail blood. For oral glucose tolerance testing, mice were trained to voluntarily consume a bolus of glucose delivered via gelatin vehicle as previously described (Zhang, 2011). Briefly, glucose gelatins were prepared by mixing solutions of 14% gelatin (Kroger Co.) and 75% glucose (Sigma-Aldrich, St. Louis, MO) in water. One well of a 24-well tissue culture plate was used as a mold for one glucose gelatin containing 0.9g of glucose. The solution was allowed to set overnight at 4°C. Mice were conditioned to voluntarily consume a small piece of glucose gelatin over a period of 4 days. On the evening prior to the first day, each animal was singly housed and subjected to an overnight fast (approximately 20 hrs). At the end of the fast, each mouse was presented with a piece of glucose gelatin (approximately 1/8 of one whole glucose gelatin) and was re-fed with normal chow once the entire piece was consumed. For the next three days, a piece of glucose gelatin was given at the same time of day (without prior fasting). Following the end of the 3-day conditioning period, the oral glucose tolerance test (OGTT) was performed. For the OGTTT, mice were subjected to a 6 hr fast, after which basal blood glucose measurements were taken and each mouse was presented with gelatin containing a dosage equivalent to 3g glucose/kg body mass. Mice were excluded from OGGT analysis if they did not consume the entire piece of gelatin within 2

minutes of presentation. Blood glucose was measured and recorded at 15, 30, 60, 90, and 120 mins following completion of consumption of the glucose gelatin.

Measurement of Glucose, Insulin, FFA and Glycerol Response to Submaximal Exercise: Basal, 6 hr fasting blood glucose measurements were taken as described above, after which the mice were subjected to 60 min of running at 15 m/min (speed was decreased from 20 m/min used for the periodic endurance run tests in order to account for increased age at this time point) at a 10° incline. Immediately following running, blood glucose was measured from tail blood with a glucose meter (TRUEtest, Walgreen Co.), and up to 200µl of blood was collected via submandibular puncture for glycerol, FFA and insulin analyses. The sample was allowed to clot at room temperature for 20 mins, spun at 2,000g for 10 min at 4°C to remove the clot, and the serum supernatant was transferred to a new tube and stored at -80°C until further analysis. Insulin was measured via ELISA (Crystal Chem, Inc., Downers Grove, IL) according to the manufacturer's instructions. Glycerol and FFA were measured using a plate-based assay (Zen-Bio, Inc., Research Triangle Park, NC) according to the manufacturer's instructions. Optical densities for these assays were determined with a microplate reader (BioRad Model 550, Global Medical Instrumentation Inc., Ramsey, MN). Basal fasting serum was collected from each animal as described above several days prior to running and analyzed at the same time of day as post-exercise serum.

Tissue Collection and Processing: At 45 weeks of age, mice were anesthetized via intraparitoneal injection of a Ketamine/Xylazine cocktail (Ketaject 100mg/kg, Xylazine 5mg/kg) and sacrificed for collection of adipose, skeletal muscle, and various organ tissues. Tissues were excised, weighed, and flash frozen in liquid nitrogen unless otherwise noted. Portions of WAT (extracted from gonadal region) and BAT (interscapular region) were fixed in 10% neutral

buffered formalin for 72 hours at 4°C in preparation for histological analysis. The triceps surae muscles from one leg of each mouse were dissected, trimmed to obtain the mid-belly portion, mounted in a transverse position on a cork base using OCT tissue freezing medium, and flash frozen in liquid nitrogen-cooled isopentane. To obtain a subsarcolemmal mitochondrial sub-population, quadriceps femoris muscles from each leg of male adipoVEGF-/- and control mice were excised, weighed, immediately placed in 1.75mL/sample freshly prepared, cold Chappell-Perry buffer (100 mM potassium chloride, 50mM 3-(N-morpholino)propanesulfonic acid, 1mM ethylene glycol tetraacetic acid, 10mM magnesium sulfate, 1mM adenosine triphosphate, pH 7.4) supplemented with a protease inhibitor cocktail (BioVision, Inc. #K271-500), and finely minced with scissors. Both quadriceps muscles from each animal were used for mitochondrial assessment. Each sample was disrupted with a Potter-Elvehjem homogenizer and centrifuged at 800g for 10 min at 4°C a total of 3 times to remove debris. The final supernatant was spun at 10,000g for 10 min at 4°C. The pellet was rinsed, resuspended in Chappell-Perry buffer, spun again at 10,000g for 10 min at 4°C, rinsed with phosphate-buffered saline and resuspended in RIPA buffer (Sigma-Aldrich, St. Louis, MO). Total protein concentrations were determined using the Lowry method according to the manufacturer's instructions (DC™ Protein Assay, Bio-Rad, Hercules, CA). With the exception of adipose tissue preserved in 10% neutral buffered formalin, all samples were stored at -80°C until further processing.

Histochemistry and Image Analysis: To assess adipose tissue capillarity, fixed WAT and BAT was processed to paraffin blocks, cut into 5μm sections, mounted on glass slides and stained with CD31 antibody for endothelial cell labeling (1:50, ab28364, abcam, Cambridge, UK). Using light microscopy (Zeiss primo star, Zeiss, Oberkochen, Germany), images were taken at 40x magnification for BAT and 20x for WAT (Axiocam IC c3, Axiovision 4.8.2.0,

Zeiss, Oberkochen, Germany). Up to 10 random, non-overlapping images were captured from each sample. Using Matlab (Version r14), the capillary-to-adipocyte ratio (C:A) in WAT was determined by dividing the total number of capillaries by the total number of adipocytes in each image. For BAT, capillary density for each image was determined by dividing the total number of capillaries counted by the area of tissue contained by that field of view. To assess skeletal muscle capillarity, frozen soleus (SOL) and plantaris (PLT) muscles embedded in tissue freezing medium were cut into 8μm transverse cryosections and placed on glass slides. Tissues were stained using the alkaline phosphatase and dipeptidylpeptidase capillary staining method (Mrázková *et al.*, 1986) and imaged at 20x magnification as described above, with the exception that successive, non-overlapping images were taken to capture the entire area of each muscle. Capillary-to-fiber ratio (C:F) was determined by counting the total number of capillaries and dividing by the total number of muscle fibers in each image using Matlab.

Protein Analysis: Basal protein expression of CPT1β and protein oxidation were analyzed using western blotting. Samples of isolated subsarcolemmal mitochondria in RIPA buffer were passed through a 27G needle 10 times. For CPT1β, 20ug of total protein were reduced, denatured, separated using SDS-PAGE gel electrophoresis, transferred to a nitrocellulose membrane, stained with Ponceau S (Boston BioProducts, Ashland, MA) and imaged. Ponceau S stain was neutralized with 0.1M NaOH and the membrane was rinsed in deionized water and then tris-buffered saline with 0.05% Tween-20 (TBST) before blocking with 5% non-fat dry milk (NFDM) in TBST, and exposed to primary (1:200, H-120: sc-20670, Santa Cruz Biotechnology, Santa Cruz, CA) and secondary (1:1000, anti-rabbit IgG HRP-linked #7074, Cell Signaling Technology, Danvers, MA) antibodies diluted in 1% NFDM in TBST. Chemiluminescent detection was carried out using ECL blotting substrate (Denville Scientific,

Inc., South Plainfield, NJ) and images were captured using Genesnap software (version 7.01) from a digital imager (G-Box Chemi16, Syngene, Cambridge, UK). Protein expression was quantified using NIH ImageJ software (version 1.46r) and represented as optical density in arbitrary units (AU), normalized to total protein obtained from Ponceau S staining. For analysis of protein oxidation, the OxyBlot™ Protein Oxidation Detection Kit (EMD Milipore, Billerica, MA) was used according to the manufacturer's instructions. Chemiluminescent detection and quantification of protein oxidation was carried out as described above, with the exception that the membrane was stripped of primary and secondary antibodies using Restore™ Western Blot Stripping Buffer (Pierce Biotechnology, Rockford, IL), stained with Ponceau S and imaged to obtain measurement of total protein *after* initial probing and imaging of signal indicating protein oxidation.

Statistical Analyses: All data are presented as mean ± SEM. Statistical analyses were carried out using Statview Statistical Software package (v5.0.01, SAS Institute Inc., Cary, NC). Significance was accepted at an α of $p<0.05$. When comparing adipoVEGF vs. control mice for VEGF expression, tissue capillarity, CPT1β expression, and oxidative damage, a student's t test was used. For examining effect of genotype and sex on tissue masses, a 2-way ANOVA was used. A repeated measures ANOVA (rANOVA) was used to analyze body mass, percent body fat, endurance running capacity and maximal running speed, glucose tolerance, and response of glucose, insulin, glycerol, and FFA to exercise. Where a main effect was observed, post hoc testing was performed using student's t tests. Student's unpaired t tests were used to compare adipoVEGF-/- to control mice for a given condition or at a given time-point. When examining the effect of exercise on a circulating factor (i.e. glucose, insulin, glycerol, or FFA) within the same grouping of mice, student's paired t tests were used.

RESULTS

Tissue VEGF expression and capillarity. Detection of the Cre transgene in tail snip DNA from adipoVEGF-/- mice was confirmed by a PCR product of 380 base pairs (Figure 1A, lane 1), while this product was absent in control samples (Figure 1A, lane 2). All experimental animals were homozygous positive for presence of LoxP sites, indicated by a PCR product at 150 base pairs (Figure 1B, lane 1). AdipoVEGF-/- mice showed a PCR product of 670 base pairs in WAT and BAT indicating deletion between LoxP sites in genomic DNA, while this band was absent in WAT and BAT from control mice and skeletal muscle of both adipoVEGF-/- and control mice (Figure 1C). Presence of VEGF mRNA (corresponding to a sequence between the LoxP floxed region) was indicated by a PCR product at 160 base pairs (Figure 1D). AdipoVEGF-/- mice showed a 50% decrease in VEGF mRNA expression in WAT, and a 90% decrease in BAT ($p<0.01$), and no difference in VEGF mRNA expression in skeletal muscle (Figure 1E).

For tissue capillarity, adipoVEGF-/- mice showed a 40% decrease in C:A in WAT ($p<0.01$, Figure 2C), and a 40% decrease in capillary density in BAT ($p<0.05$, Figure 2D) compared to controls. There was no difference in C:F of either PLT or SOL tissue (Figure 2E and 2F).

Animal body mass, body fat, and tissue characteristics. Body mass in adipoVEGF-/- mice was significantly different at 24 weeks old ($p<0.05$, Figure 3A) and displayed a significant main effect for sex. Male adipoVEGF-/- mice showed decreased body mass compared to controls at all time-points ($p<0.05$, Figure 3B), while there was no difference in body mass in female mice (Figure 3C). When combining males and females, percentage body fat was significantly decreased in adipoVEGF-/- mice at 12 and 24 weeks old ($p<0.05$, Figure 3D). In males, adipoVEGF-/- mice showed significantly decreased percentage body fat at 12 weeks ($p<0.05$,

Figure 3E), while the same effect was seen in females at 24 weeks (Figure 3F). Overall, there was a trend towards decreased body mass and percentage body fat in adipoVEGF-/- mice compared to controls.

At the time of sacrifice at 45 weeks old, control WAT tissue mass was two times greater ($p<0.05$) and control BAT tissue mass was three times greater ($p<0.0001$) than adipoVEGF-/- mice (Table 1). A similar effect on WAT and BAT tissue mass was observed when considering male and female groups separately, with the exception that the increase in female control WAT mass was not statistically significant (Table 2). When comparing males to females of the same genotype, adipoVEGF-/- and control males had a greater heart mass than their female counterparts ($p<0.05$), and control males had a greater soleus mass than control females ($p<0.05$, Table 2).

Endurance and maximal running speed performance. When subjected to submaximal exercise capacity testing, adipoVEGF-/- mice showed a significant 30% decrease (rANOVA $p<0.001$) in time to exhaustion compared to controls (Figure 4A). There was no difference in the age-associated rate of decline between the groups; both adipoVEGF-/- and control mice showed a similar 37% decline in time to exhaustion from the age of 6 to 24 wks. There was no difference in maximal running speed between adipoVEGF-/- and control mice and both groups showed a similar age-related decline (Figure 4B).

Response to oral glucose tolerance testing. There were no significant differences in blood glucose levels at any time-point during an oral glucose tolerance test (Figure 5).

Response of circulating substrates to submaximal exercise. Combining males and females, no difference was observed in basal blood glucose levels. In response to one hour of submaximal exercise, there was a significant drop in blood glucose in both adipoVEGF-/- and

control mice ($p<0.01$). AdipoVEGF-/- mice exhibited a trend towards decreased post-exercise blood glucose compared to controls (rANOVA $p=0.06$, Figure 6A). In males, post-exercise blood glucose was significantly decreased compared to basal in control mice ($p<0.01$), and a trend towards the same effect was observed in adipoVEGF-/- males ($p=0.06$, Figure 6B). No differences were observed in female basal or post-exercise blood glucose (Figure 6C). Basal insulin was significantly decreased in adipoVEGF-/- mice compared to controls ($p<0.05$), and was decreased in response to exercise ($p<0.01$) in both groups in all cases (all, male, and female mice, Figure 6D-E). When combining male and female data, insulin was significantly decreased in adipoVEGF-/- mice compared to controls ($p<0.05$, Figure 6D and 6E), this did not hold true for female-only data (Figure 6F). Post-exercise circulating glycerol was significantly decreased in all adipoVEGF-/- mice compared to controls ($p<0.01$, Figure 6G), and there was a trend towards decreased post-exercise circulating FFA in adipoVEGF-/- mice compared to controls ($p=0.06$, Figure 6H).

Protein expression and oxidation in skeletal muscle mitochondria. There were no significant differences in protein expression of CPT1β or protein oxidation in subsarcolemmal mitochondria isolated from quadriceps femoris muscles (Figure 7).

DISCUSSION

The principle finding of this study is that adipose-specific VEGF deficient mice show decreased endurance running capacity without a concurrent decrease in maximal running speed. Following one hour of sub-maximal exertion, adipoVEGF-/- mice displayed decreased circulating levels of glucose, insulin, and glycerol compared to littermate controls. These data suggest that deficits in adipose tissue vasculature are regulated by adipose derived VEGF, blunt

the availability of lipids from adipose tissue stores during endurance exercise, and affect insulin secretion and sensitivity.

Basal characteristics of adipoVEGF-/- mice

As expected, adipoVEGF-/- mice showed decreased VEGF mRNA content in WAT and BAT, but no difference in non-adipose tissue (such as skeletal muscle). The reduction of VEGF in adipocytes led to a decrease in adipose tissue capillarity (Figure 1). At the time of sacrifice, adipoVEGF-/- WAT tissue mass was reduced two-fold, and BAT was reduced three-fold compared to controls (Tables 1 and 2). At younger ages (6 weeks), no differences in percentage body fat were observed, but by 24 weeks, percentage body fat was significantly lower in adipoVEGF-/- mice. However, the difference in body fat percentage was not nearly as dramatic as the difference seen in individual adipose tissue masses and did not reach statistical significance at many time points (Figure 3). This discrepancy could be due to the lapse in age when these measurements were taken (tissue masses collected at 45 weeks old), however could also be affected by varied distribution of body fat between the groups. Regardless, these data are in agreement with the findings of Sung et al. (2013), that adipoVEGF-/- mice show little difference in body mass, a small decrease in body fat percentage, and dramatic decrease in gonadal fat tissue mass under basal conditions. Collectively, these data suggest that adipose-specific VEGF deficiency reduces WAT mass at the gonadal and BAT at interscapular regions. Although adiposity is decreased in adipoVEGF-/- mice, adipose tissue lacking the angiogenic effects of VEGF is found to be hypoxic, inflammatory, metabolically dysfunctional, especially under conditions such as high fat feeding (Sun *et al.*, 2012; Sung *et al.*, 2013). This points to stimulation of adipose tissue angiogenesis as a potential therapeutic intervention in metabolic diseases.

Response to endurance and maximal exercise

AdipoVEGF-/- mice displayed decreased endurance running capacity, without a concurrent decrease in maximal running speed (Figure 4). This suggests an alteration in substrate availability or utilization in adipoVEGF-/- mice, rather than a change in maximal oxygen uptake capacity. To test this, we measured circulating glucose, insulin, glycerol and FFA under basal, fasted conditions and again immediately following one hour of submaximal exercise (Figure 6). In control animals, the response of these metabolites to the given intensity and duration of exercise was physiologically appropriate, i.e. glucose and insulin fell and FFA and glycerol were elevated at the end of the exercise bout (Zinker *et al.*, 1990). In response to exercise, glucose displayed a trending decrease and insulin and glycerol were significantly decreased in adipoVEGF-/- mice. Notably, glycerol trended downward in response to exercise in adipoVEGF-/- mice, but increased over this duration in control animals. Similar results were seen for FFA, where there was a slight trend towards increasing FFA during exercise in adipoVEGF-/- mice, while FFA was significantly increased in controls over this duration (Figure 6). Post-exercise FFA was down in adipoVEGF-/- mice compared to controls. Overall, these data suggest that adipoVEGF-/- mice were unable to mobilize lipid-derived substrate into the bloodstream to the same degree as littermate controls during submaximal exercise.

We speculate that the inability to mobilize lipid-derived energy during submaximal exercise is due to decreased perfusion of the adipose tissue as a result of VEGF deficiency and reduced adipose vascularity. This could be due to an inability to move FFA into the bloodstream and/or carry FFA away from the tissue once released from adipocytes.

It is well accepted that insulin secretion is blunted during prolonged low intensity exercise to allow for lipolysis (Wasserman *et al.*, 1989). This could also explain the post-

exercise deficit in insulin in adipoVEGF-/- mice compared to controls. If lipid substrates are not made available at an appropriate rate during exercise, this may elicit a feedback loop to further suppress insulin secretion in order to increase lipolysis and stimulate an increase in circulating FFA. Interestingly, basal fasting insulin was also decreased in adipoVEGF-/- mice compared to controls (Figure 6). It is plausible that this decrease serves to raise FFA under conditions of comprised ability to mobilize them at rest, as well. Quantification of HSL phosphorylation in adipose tissue under basal fasted conditions would aid in addressing this hypothesis, but was not performed in this study. Additionally, no difference was observed in OGTT handling under basal conditions (Figure 5). Equivalent fasting blood glucose and handling of an OGTT, accompanied by an overall decrease in fasting insulin suggests an increase in skeletal muscle insulin sensitivity in adipoVEGF-/- mice. These observations suggest that the skeletal muscles of adipoVEGF-/- mice may be adapting and becoming more efficient and insulin sensitive to make up for deficiencies in lipid substrate availability.

Skeletal muscle characteristics of adipoVEGF-/- mice

To rule out the possibility of adipose tissue modification leading to an unintended effect skeletal muscle capillarity, we confirmed that there was no difference in muscle capillarity in PLT and SOL muscle (Figure 2). The DNA deletion band was not present and there was no difference in levels of VEGF mRNA expression in skeletal muscle of adipoVEGF-/- mice (Figure 1). Protein expression of CPT1β in subsarcolemmal mitochondria isolated from the quadriceps femoris was measured in attempt to gauge differences in fatty acid oxidation between the groups, which could also be associated with deficits in endurance exercise capacity (Figure 7). Compared to littermate controls, no differences were observed in CPT1β protein expression in the skeletal muscle of adipoVEGF-/- mice. Future quantification of fatty acid translocase

(CD36) expression may be helpful in examining differences in lipid transport into muscle cells and mitochondria of adipoVEGF-/- mice. General protein oxidation was also measured to determine whether oxidative damage occurred within the muscles of adipoVEGF-/- mice (Figure 6). However, no difference was observed. Overall, based on the present findings, it seems unlikely that the difference in endurance running capacity can be attributed to muscle capillarity and/or skeletal muscle mitochondrial dysfunction.

Interpretation and significance

Elevated circulating levels of VEGF have been shown in obese individuals and studies have investigated the prospect of inhibiting VEGF action in adipose tissue as a means of treating obesity (Kolonin *et al.*, 2004; Cao, 2010; Wada *et al.*, 2011). However, our findings suggest an important role for adipose VEGF and maintenance of appropriate substrate availability during submaximal exertion, through the regulation of adipose tissue vasculature. Our data support the notion that adipose VEGF is essential for the maintenance of adipose tissue health and metabolic homeostasis (Sun *et al.*, 2012; Elias *et al.*, 2012; Sung *et al.*, 2013; Shimizu *et al.*, 2014). Gaining a more specific and quantitative understanding of direct FFA release into circulation from adipose tissue and lipid uptake by working skeletal muscle in adipoVEGF-/- mice could be important in developing effective therapeutic manipulations of the VEGF pathway in conjunction with exercise-based therapies. For example, the condition of adipose tissue in adipoVEGF-/- mice is similar to what is observed in human adipose tissue during obesity, such that it is undervascularized, hypoxic and inflammatory (Sun *et al.*, 2011; Sung *et al.*, 2013). Therefore, the notion that reductions in adipose capillarity can affect substrate availability during submaximal exercise could be applied to diet and exercise prescription targeted at the treatment

of obesity. Additionally, this may influence considerations for anti-VEGF therapies along with diet and exercise prescription in cancer patients and survivors.

In conclusion, adipose VEGF is an important regulator of adipose tissue capillarity, which affects metabolic function during prolonged, submaximal exercise conditions. In agreement with our hypothesis, adipose VEGF plays an important role in the availability of lipid-derived substrate availability during endurance exercise. The body may attempt to compensate for dysregulation caused by deficits in adipose tissue vasculature through decreased insulin secretion and increased skeletal muscle insulin sensitivity and efficiency.

REFERENCES

Baynard T, Vieira-Potter VJ, Valentine RJ & Woods J a (2012). Exercise training effects on inflammatory gene expression in white adipose tissue of young mice. *Mediators Inflamm* **2012,** 767953.

Cao Y (2010). Adipose tissue angiogenesis as a therapeutic target for obesity and metabolic diseases. *Nat Rev Drug Discov* **9,** 107–115.

Elias I, Franckhauser S, Ferré T, Vilà L, Tafuro S, Muñoz S, Roca C, Ramos D, Pujol A, Riu E, Ruberte J & Bosch F (2012). Adipose tissue overexpression of vascular endothelial growth factor protects against diet-induced obesity and insulin resistance. *Diabetes* **61,** 1801–1813.

Gerber HP, Hillan KJ, Ryan AM, Kowalski J, Keller GA, Rangell L, Wright BD, Radtke F, Aguet M & Ferrara N (1999). VEGF is required for growth and survival in neonatal mice. *Development* **126,** 1149–1159.

Hatano D, Ogasawara J, Endoh S, Sakurai T, Nomura S, Kizaki T, Ohno H, Komabayashi T & Izawa T (2011). Effect of exercise training on the density of endothelial cells in the white adipose tissue of rats. *Scand J Med Sci Sports* **21,** e115–21.

Høydal MA, Wisløff U, Kemi OJ & Ellingsen O (2007). Running speed and maximal oxygen uptake in rats and mice: practical implications for exercise training. *Eur J Cardiovasc Prev Rehabil* **14,** 753–760.

Kolonin MG, Saha PK, Chan L, Pasqualini R & Arap W (2004). Reversal of obesity by targeted ablation of adipose tissue. *Nat Med* **10,** 625–632.

Koves TR, Ussher JR, Noland RC, Slentz D, Mosedale M, Ilkayeva O, Bain J, Stevens R, Dyck JRB, Newgard CB, Lopaschuk GD & Muoio DM (2008). Mitochondrial overload and incomplete fatty acid oxidation contribute to skeletal muscle insulin resistance. *Cell Metab* **7,** 45–56.

Leung DW, Cachianes G, Kuang WJ, Goeddel D V & Ferrara N (1989). Vascular endothelial growth factor is a secreted angiogenic mitogen. *Science* **246,** 1306–1309.

Malek MH & Olfert IM (2009). Global deletion of thrombospondin-1 increases cardiac and skeletal muscle capillarity and exercise capacity in mice. *Exp Physiol* **94,** 749–760.

Mrázková O, Grim M & Carlson BM (1986). Enzymatic heterogeneity of the capillary bed of rat skeletal muscles. *Am J Anat* **177,** 141–148.

Olfert IM, Howlett R a, Tang K, Dalton ND, Gu Y, Peterson KL, Wagner PD & Breen EC (2009). Muscle-specific VEGF deficiency greatly reduces exercise endurance in mice. *J Physiol* **587,** 1755–1767.

Olfert IM, Howlett R a, Wagner PD & Breen EC (2010). Myocyte vascular endothelial growth factor is required for exercise-induced skeletal muscle angiogenesis. *Am J Physiol Regul Integr Comp Physiol* **299,** R1059–67.

Samuel VT, Petersen KF & Shulman GI (2010). Lipid-induced insulin resistance: unravelling the mechanism. *Lancet* **375,** 2267–2277.

Shimizu I, Aprahamian T, Kikuchi R, Shimizu A, Papanicolaou KN, MacLauchlan S, Maruyama S & Walsh K (2014). Vascular rarefaction mediates whitening of brown fat in obesity. *J Clin Invest* **124,** 2099–2112.

Sun K, Kusminski CM & Scherer PE (2011). Adipose tissue remodeling and obesity. *J Clin Invest* **121,** 2094–2101.

Sun K, Wernstedt I, Kusminski CM, Carolina A, Wang Z V, Pollard JW, Brekken RA & Scherer PE (2012). Dichotomous effects of VEGF-A on adipose tissue dysfunction. *Proc Natl Acad Sci* **109,** 5874–5879.

Sung H-K, Doh K-O, Son JE, Park JG, Bae Y, Choi S, Nelson SML, Cowling R, Nagy K, Michael IP, Koh GY, Adamson SL, Pawson T & Nagy A (2013). Adipose vascular endothelial growth factor regulates metabolic homeostasis through angiogenesis. *Cell Metab* **17,** 61–72.

Wada H, Ura S, Kitaoka S, Satoh-Asahara N, Horie T, Ono K, Takaya T, Takanabe-Mori R, Akao M, Abe M, Morimoto T, Murayama T, Yokode M, Fujita M, Shimatsu A & Hasegawa K (2011). Distinct characteristics of circulating vascular endothelial growth factor-a and C levels in human subjects. *PLoS One* **6,** e29351.

Wasserman DH, Lacy DB, Goldstein RE, Williams PE & Cherrington AD (1989). Exercise-induced fall in insulin and increase in fat metabolism during prolonged muscular work. *Diabetes* **38,** 484–490.

Zhang L (2011). Voluntary oral administration of drugs in mice. *Protoc Exch*1–12.

Zinker BA, Britz K & Brooks GA (1990). Effects of a 36-hour fast on human endurance and substrate utilization. *J Appl Physiol* **69,** 1849–1855.

ADDITIONAL INFORMATION

Competing Interests

None declared.

Author Contributions

I.M.O. conceived the project and N.J.Z. and L.V.D helped to design the study. N.J.Z., G.C.O., J.C.S., and J.A. conducted the experiments and collected data. N.J.Z. and I.M.O. participated in writing the manuscript, and all authors contributed in editing and approving the manuscript.

Funding

This project was supported by funding from the West Virginia University Mary Babb Randolph Cancer Center American Cancer Society- IRG 1005460R (I.M.O), WV-INBRE NIH P20GM103434 (J.A.), and the West Virginia University Research Corporation PSCoR Grant (I.M.O, L.V.D.).

Acknowledgements

The authors would like to thank Kyle Mandler for his assistance in collecting tissue samples and Gavin Washington for his assistance in collecting data.

Table 1. Body and tissue masses- all mice at 45 wks old (mean ± SEM)

	All		Main Effect p Value	
	adipoVEGF-/-	Control	Genotype	Sex
	n=10	n=11		
Body mass (g)	25.8 ± 1.1	29.3 ± 1.3	n.s. (0.1)	0.06
Heart mass (mg)	109.1 ± 5.3	120.1 ± 6.0	n.s.	<0.001
Heart mass/body mass (mg/g)	4.2 ± 0.2	4.1 ± 0.1	n.s.	<0.05
Spleen mass (mg)	78.4 ± 9.3	130.3 ± 23.3	n.s.	n.s.
Spleen mass/body mass (mg/g)	3.1 ± 0.4	4.3 ± 0.6	n.s.	n.s.
WAT mass (mg)	586.3 ± 103.8**	1099.3 ± 130.0	<0.05	n.s.
WAT mass/body mass (mg/g)	22.2 ± 2.8**	36.5 ± 3.5	<0.01	n.s.
BAT mass (mg)	32.5 ± 5.1**	106.4 ± 10.2	<0.0001	n.s.
BAT mass/body mass (mg/g)	1.2 ± 0.2**	3.6 ± 0.3	<0.0001	n.s.
Gastrocnemius mass (mg)	108.4 ± 3.8	115.8 ± 3.6	n.s.	<0.01
Gastrocnemius mass/body mass (mg/g)	4.2 ± 0.1	4.0 ± 0.1	n.s.	n.s.
Soleus mass (mg)	6.9 ± 0.8	6.4 ± 0.6	n.s.	<0.05
Soleus mass/body mass (mg/g)	0.3 ± 0.03	0.2 ± 0.01	n.s.	n.s.
Plantaris mass (mg)	16.8 ± 1.3	17.6 ± 1.4	n.s.	n.s.
Plantaris mass/body mass (mg/g)	0.7 ± 0.05	0.6 ± 0.06	n.s.	n.s.

Main effect p values for 2-way ANOVA. **p<0.01, comparing adipoVEGF-/- to littermate controls

Table 2. Body and tissue masses- male and female mice at 45 wks old (mean ± SEM)

	Male		Female	
	adipoVEGF-/-	Control	adipoVEGF-/-	Control
	n=5	n=7	n=5	n=4
Body mass (g)	27.0 ± 1.2	30.9 ± 1.4	24.6 ± 1.9	26.6 ± 2.2
Heart mass (mg)	122.0 ± 5.5†	130.2 ± 6.3†	96.1 ± 3.3	102.4 ± 5.3
Heart mass/body mass (mg/g)	4.5 ± 0.2	4.2 ± 0.2	4.0 ± 0.2	3.9 ± 0.2
Spleen mass (mg)	67.8 ± 7.0	134.1 ± 36.3	88.9 ± 16.9	123.6 ± 18.2
Spleen mass/body mass (mg/g)	2.5 ± 0.3	4.2 ± 0.9	3.6 ± 0.7	4.6 ± 0.4
WAT mass (mg)	582.2 ± 78.1*	1122.1 ± 133.7	589.6 ± 187.4	1059.5 ± 302.5
WAT mass/body mass (mg/g)	21.7 ± 2.2*	35.8 ± 3.3	22.5 ± 5.0	37.8 ± 8.6
BAT mass (mg)	39.2 ± 7.1**	115.9 ± 11.7	25.7 ± 6.7**	89.8 ± 17.9
BAT mass/body mass (mg/g)	1.4 ± 0.2**	3.8 ± 0.4	1.0 ± 0.2**	3.3 ± 0.5
Gastrocnemius mass (mg)	115.4 ± 3.2	120.7 ± 2.4	101.4 ± 5.6	107.1 ± 7.5
Gastrocnemius mass/body mass (mg/g)	4.3 ± 0.1	3.9 ± 0.2	4.1 ± 0.1	4.1 ± 0.2
Soleus mass (mg)	7.9 ± 1.4	7.2 ± 0.6†	5.8 ± 0.5	5.0 ± 0.7
Soleus mass/body mass (mg/g)	0.3 ± 0.05	0.2 ± 0.02	0.2 ± 0.02	0.2 ± 0.02
Plantaris mass (mg)	17.7 ± 2.6	19.1 ± 1.9	15.9 ± 0.5	14.9 ± 0.9
Plantaris mass/body mass (mg/g)	0.7 ± 0.1	0.6 ± 0.1	0.7 ± 0.03	0.6 ± 0.02

**p<0.01, *p<0.05 comparing adipoVEGF-/- to littermate controls within the same sex, †p<0.05 comparing males to females within the same genotype

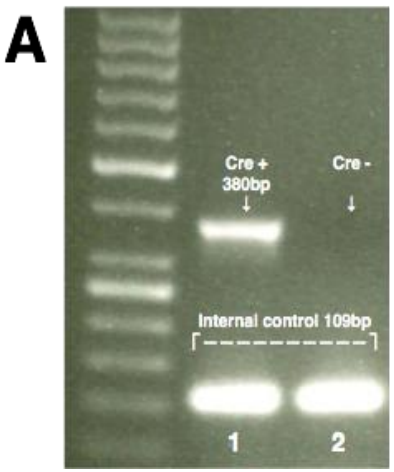
A
Cre +
380bp
Cre -
Internal control 109bp
1
2

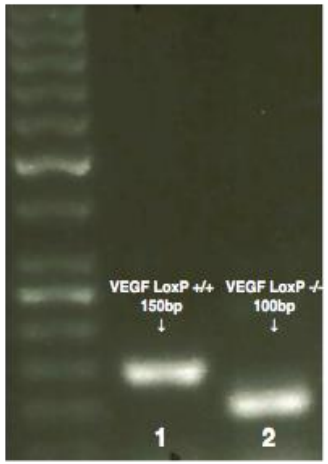
B
VEGF LoxP +/+
150bp
VEGF LoxP -/-
100bp
1
2

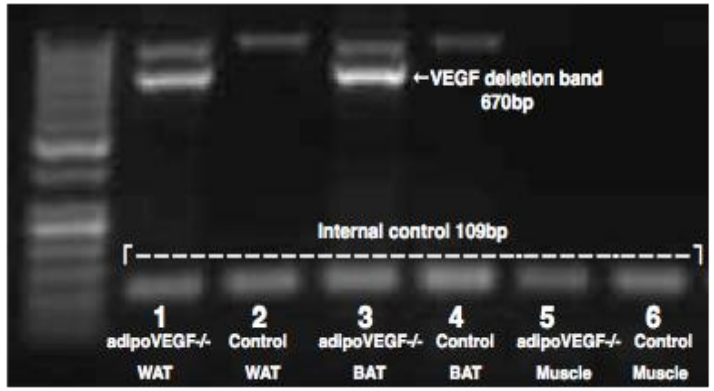
C
←VEGF deletion band
670bp
Internal control 109bp
1 adipoVEGF-/- WAT
2 Control WAT
3 adipoVEGF-/- BAT
4 Control BAT
5 adipoVEGF-/- Muscle
6 Control Muscle

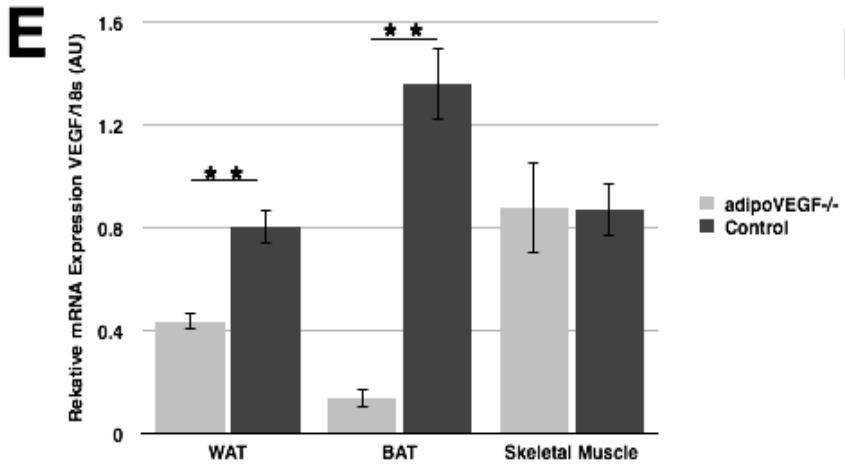
E
Rekative mRNA Expression VEGF/18s (AU)
1.6
1.2
0.8
0.4
0
* *
* *
WAT
BAT
Skeletal Muscle
adipoVEGF-/-
Control

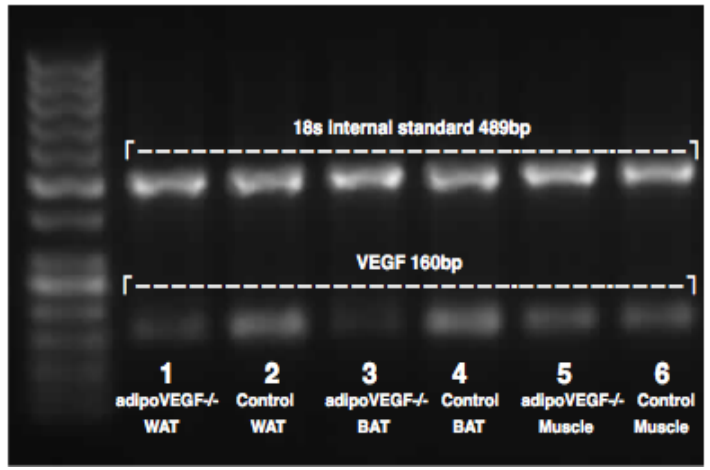
D
18s internal standard 489bp
VEGF 160bp
1 adipoVEGF-/- WAT
2 Control WAT
3 adipoVEGF-/- BAT
4 Control BAT
5 adipoVEGF-/- Muscle
6 Control Muscle

Figure 1. DNA and mRNA expression of VEGF in adipose and skeletal muscle tissue of adipoVEGF-/- vs. littermate control mice. PCR products from tail-snip DNA indicating presence (A, lane 1) and absence (A, lane 2) of the Cre transgene at 380 bp, with internal control shown at 109 bp. Homozygosity for presence of VEGF LoxP sites (+/+) indicated by a product at 150 bp (B, lane 1), while homozygosity for absence of these sites (-/-) indicated by a 100 bp product (B, lane 2). Indication of deletion in genomic DNA between LoxP sites shown by 670 bp product in adipoVEGF-/- white adipose tissue (WAT) and brown adipose tissue (BAT) (C, lanes 1 and 3 respectively) and absence of this product in control WAT and BAT (C, lanes 2 and 4 respectively). Absence of this deletion band also observed in both adipoVEGF-/- and control skeletal muscle (C, lanes 5 and 6 respectively). VEGF mRNA expression in adipoVEGF-/- WAT and BAT (D, lanes 1 and 3 respectively) indicated by a 160 bp product. Control tissues include WAT and BAT from control mice (D, lanes 2 and 4 respectively), and adipoVEGF-/- and control skeletal muscle (D, lanes 5 and 6 respectively). 18s rRNA internal standard product shown at 489 bp (D, all lanes). (E) Quantification of relative VEGF mRNA expression in indicated tissues of adipoVEGF-/- vs. control mice (n=4 per tissue, per group). Data presented as mean ± SEM, **$p<0.01$ comparing adipoVEGF-/- to control for a given tissue type.

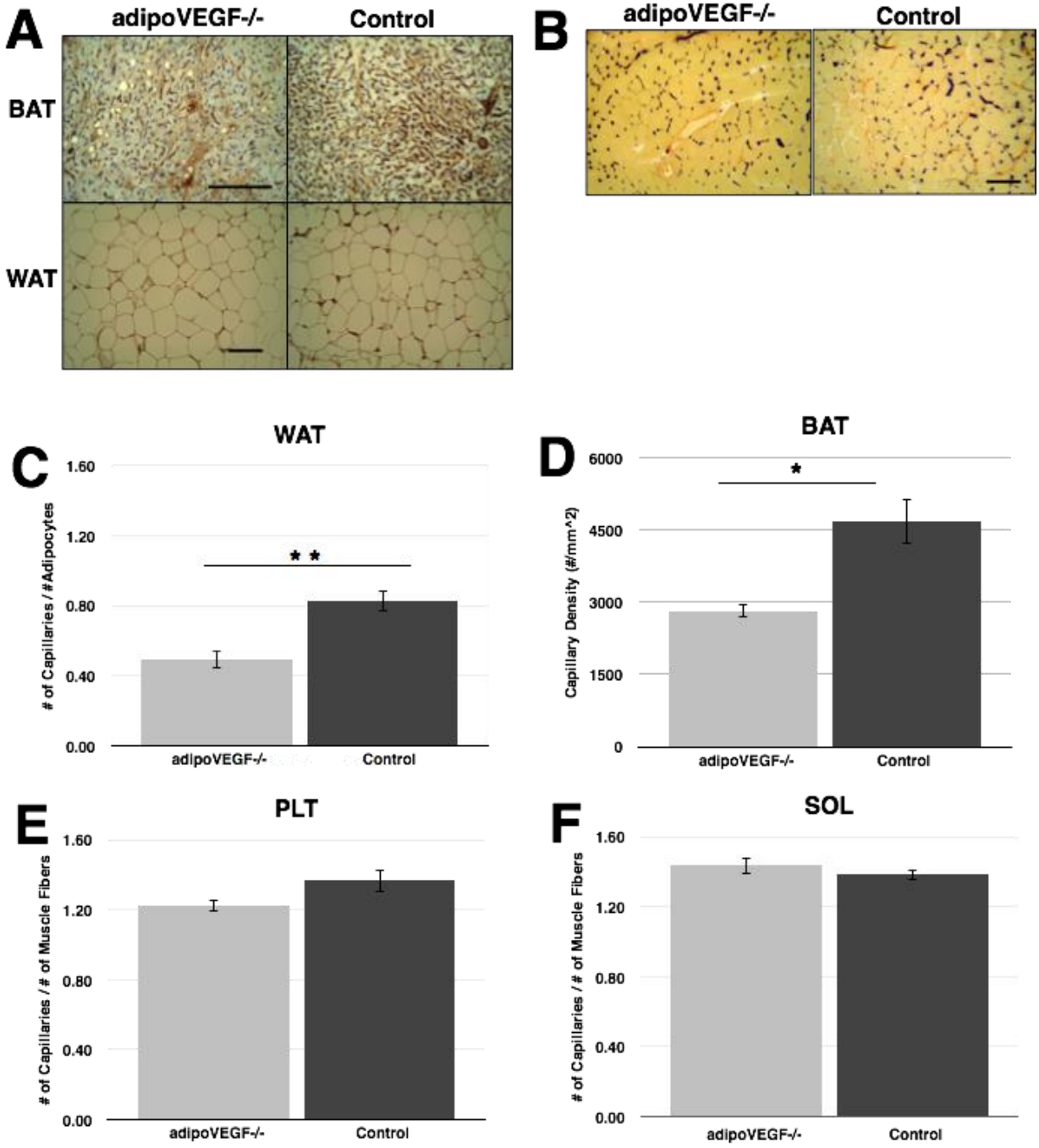
A
adipoVEGF-/-
Control
BAT
WAT
B
adipoVEGF-/-
Control
C
WAT
# of Capillaries / #Adipocytes
1.60
1.20
0.80
0.40
0.00
* *
adipoVEGF-/-
Control
D
BAT
Capillary Density (#/mm^2)
6000
4500
3000
1500
0
*
adipoVEGF-/-
Control
E
PLT
# of Capillaries / # of Muscle Fibers
1.60
1.20
0.80
0.40
0.00
adipoVEGF-/-
Control
F
SOL
# of Capillaries / # of Muscle Fibers
1.60
1.20
0.80
0.40
0.00
adipoVEGF-/-
Control

Figure 2. Capillarity in WAT, BAT, and skeletal muscle of adipoVEGF-/- vs. littermate control mice. (A) Representative images shown at 20x magnification for white adipose tissue (WAT) and 40x for brown adipose tissue (BAT). (B) Representative images shown at 20x magnification for plantaris muscle (PLT). Scale bars represent 100μm. (C) Quantification of capillary to adipocyte ratio in WAT (adipoVEGF-/- n=5, control n=4) and (D) capillary density in BAT (adipoVEGF-/- n=2, control n=4). (E) Quantification of capillary to fiber ratio in PLT and (F) soleus muscles (SOL) (adipoVEGF-/- n=9, control n=10). Data presented as mean ± SEM, **p<0.01, *p<0.

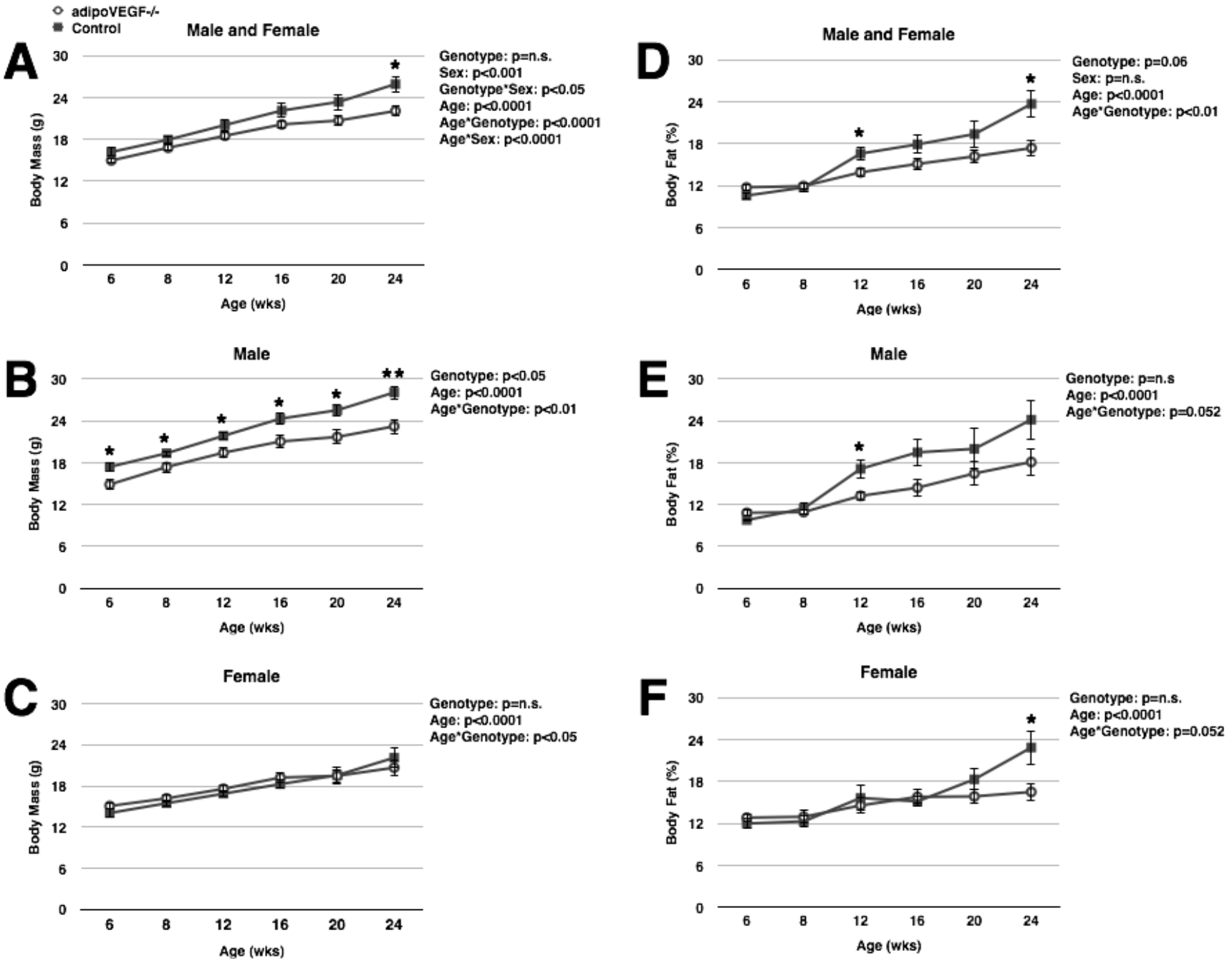
adipoVEGF-/-
Control
A
Male and Female
Body Mass (g)
Age (wks)
Genotype: p=n.s.
Sex: p<0.001
Genotype*Sex: p<0.05
Age: p<0.0001
Age*Genotype: p<0.0001
Age*Sex: p<0.0001
B
Male
Body Mass (g)
Age (wks)
Genotype: p<0.05
Age: p<0.0001
Age*Genotype: p<0.01
C
Female
Body Mass (g)
Age (wks)
Genotype: p=n.s.
Age: p<0.0001
Age*Genotype: p<0.05
D
Male and Female
Body Fat (%)
Age (wks)
Genotype: p=0.06
Sex: p=n.s.
Age: p<0.0001
Age*Genotype: p<0.01
E
Male
Body Fat (%)
Age (wks)
Genotype: p=n.s
Age: p<0.0001
Age*Genotype: p=0.052
F
Female
Body Fat (%)
Age (wks)
Genotype: p=n.s.
Age: p<0.0001
Age*Genotype: p=0.052

Figure 3. Body mass and percent body fat of adipoVEGF-/- vs. littermate control mice. Body mass (A-C) and percent body fat (D-F) in adipoVEGF-/- (n=10; male n=5, female 5) and littermate control (n=11; male =7, female=4) mice. Data presented as mean ± SEM. Main effect values reported using repeated measures ANOVA. **$p<0.01$, *$p<0.05$ comparing adipoVEGF-/- to control for a given time-point.

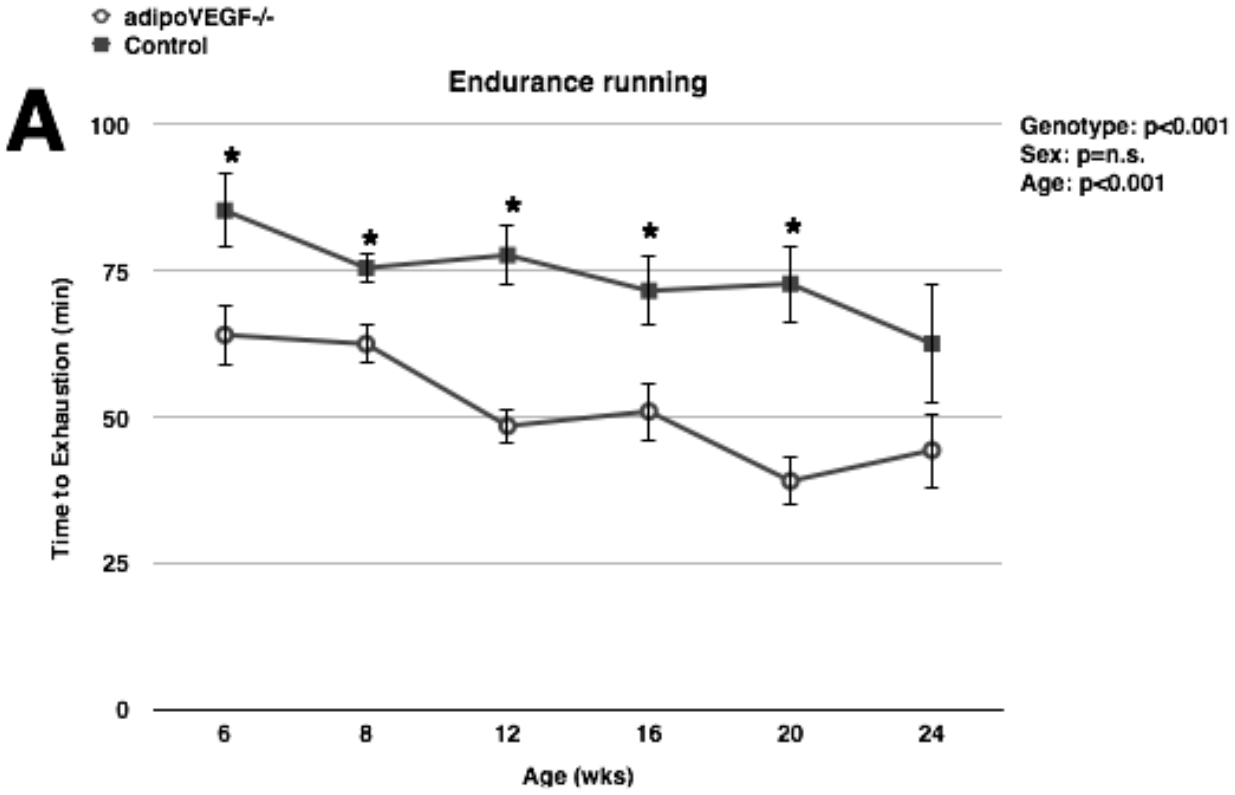
adipoVEGF-/-
Control
A
Endurance running
Genotype: p<0.001
Sex: p=n.s.
Age: p<0.001
Time to Exhaustion (min)
100
75
50
25
0
6
8
12
16
20
24
Age (wks)
*
*
*
*
*

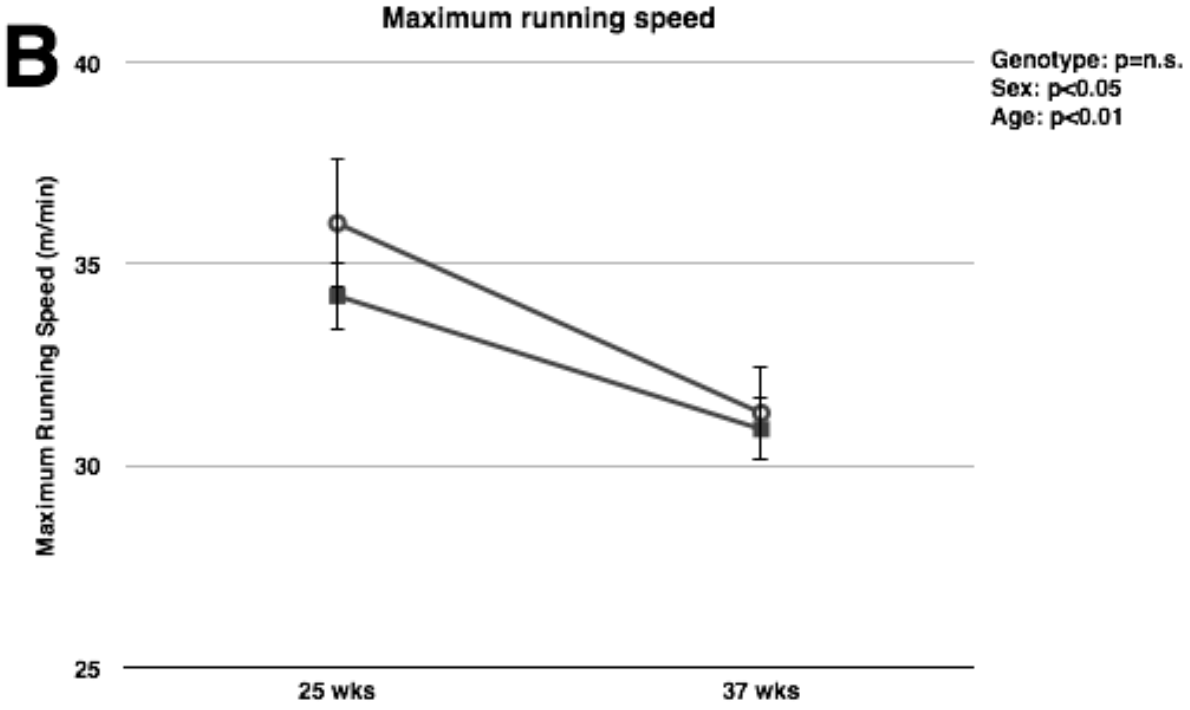
B
Maximum running speed
Genotype: p=n.s.
Sex: p<0.05
Age: p<0.01
Maximum Running Speed (m/min)
40
35
30
25
25 wks
37 wks

Figure 4. Endurance and maximal exercise capacity testing in adipoVEGF-/- vs. littermate control mice. (A) Submaximal endurance capacity and (B) maximal running speed in male and female mice (adipoVEGF-/- n=10, control n=11). For endurance running, mice ran at 20m/min at a 10° incline until exhaustion. For maximal running speed, mice ran at a 10° incline and running speed was increased by 2m/min every 30 sec until exhaustion. Data presented as mean ± SEM. Main effect values reported using repeated measures ANOVA. No significant main effect or interaction for sex was observed for endurance running. *$p<0.05$ comparing adipoVEGF-/- to control at a given time-point.

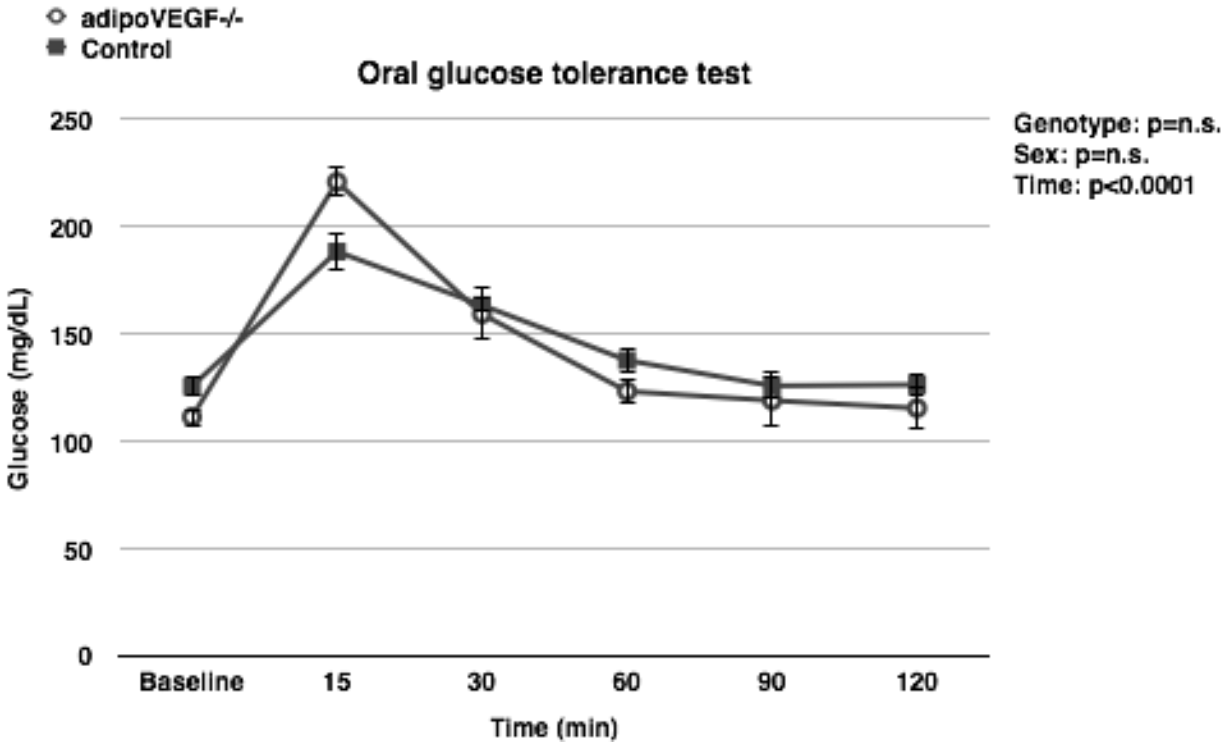
adipoVEGF-/-
Control
Oral glucose tolerance test
Genotype: p=n.s.
Sex: p=n.s.
Time: p<0.0001
Glucose (mg/dL)
250
200
150
100
50
0
Baseline
15
30
60
90
120
Time (min)

Figure 5. Oral glucose tolerance in 42-wk-old adipoVEGF-/- vs. littermate control mice. Blood glucose over the duration of an oral glucose tolerance test in male and female mice (adipoVEGF-/- n=10, control n=11). Data presented as mean ± SEM. Main effect values reported using repeated measures ANOVA. No significant main effect or interaction for sex was observed.

Genotype: p=0.06
Sex: p<0.05
Time (Exercise effect): p<0.001

adipoVEGF-/-
Control

A

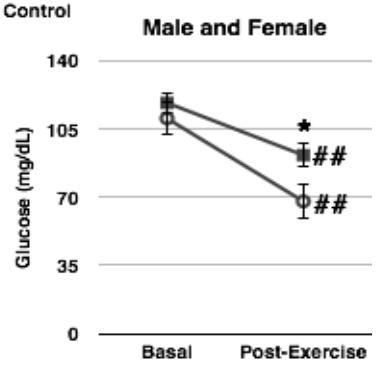

B

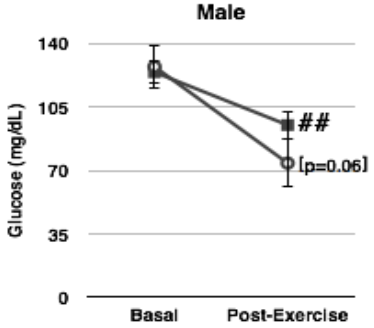

C

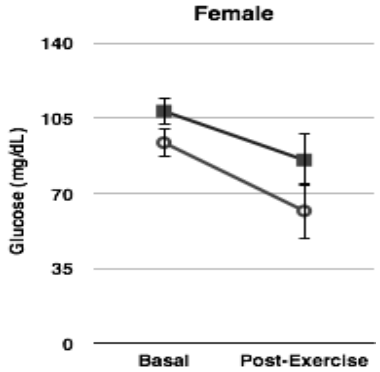

Genotype: p<0.001
Sex: p=0.06
Time (Exercise effect): p<0.0001
Time (Exercise effect)*Genotype: p<0.05
Time (Exercise effect)*Sex: p<0.01

D

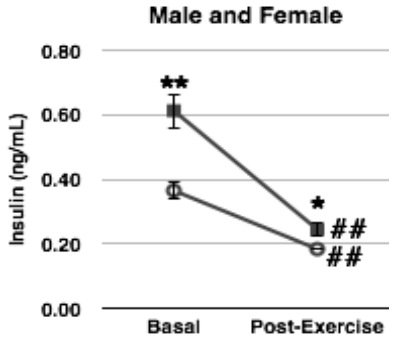

E

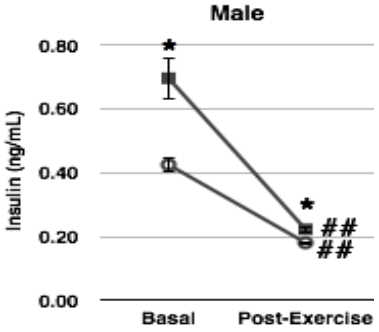

F

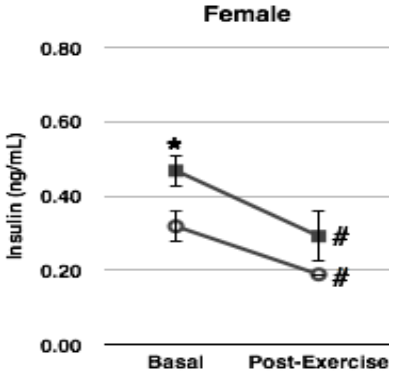

Genotype: p<0.05
Sex: p=n.s.
Time (Exercise effect): p=n.s.

G

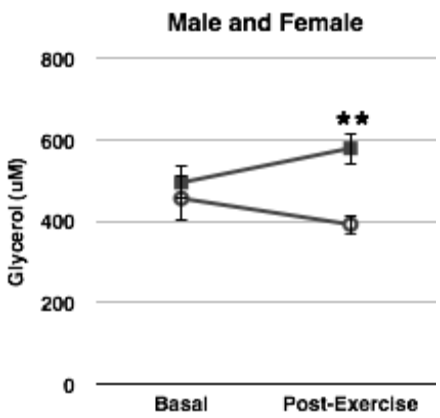

Genotype: p=n.s.
Sex: p=n.s.
Time (Exercise effect): p<0.05

H

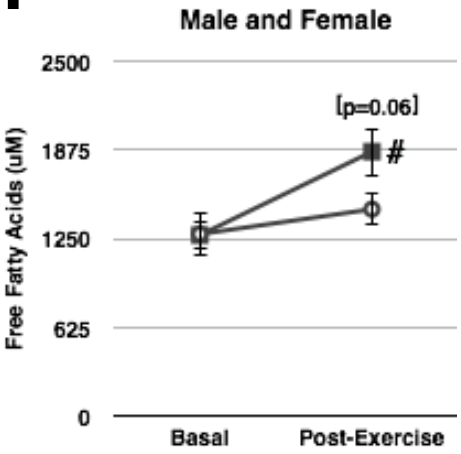

Figure 6. Submaximal exercise effect on circulating substrates in 44-wk-old adipoVEGF-/- vs. littermate control mice. Circulating basal (fasted) and post-exercise glucose (A-C) in adipoVEGF-/- (n=10; male n=5, female n=5) and littermate control (n=11; male n=7, female n=4) mice. (D-F) Insulin in males and females combined, male only and female only mice. (G) glycerol and (H) free fatty acids (FFA) in male and female mice. Exercise consisted of running at 15m/min a 10° incline for 1 hr, following a 6 hr fast. Blood glucose measurements taken from whole blood; insulin, glycerol, FFA measurements from serum. Data presented as mean ± SEM. Main effect values reported using repeated measures ANOVA. For glycerol and FFA, no significant main effect or interaction for sex was observed, therefore male and female findings are reported as combined data. **$p<0.01$, *$p<0.05$ comparing adipoVEGF-/- to control for a given condition. ##$p<0.01$, #$p<0.05$ comparing basal to post-exercise for a given genotype.

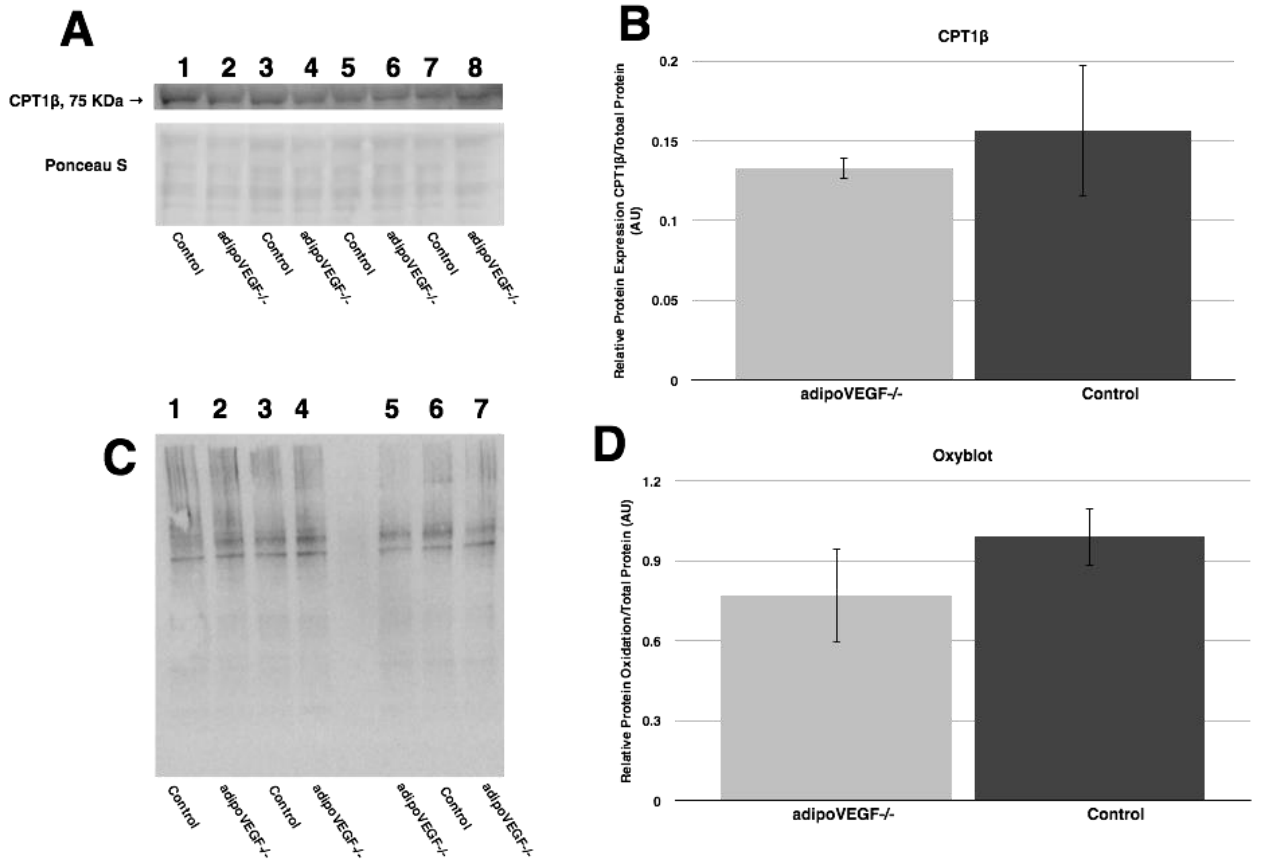
A
1 2 3 4 5 6 7 8
CPT1β, 75 KDa →
Ponceau S
Control
adipoVEGF-/-
B
CPT1β
Relative Protein Expression CPT1β/Totoal Protein (AU)
0.2
0.15
0.1
0.05
0
adipoVEGF-/-
Control
C
1 2 3 4 5 6 7
D
Oxyblot
Relative Protein Oxidation/Total Protein (AU)
1.2
0.9
0.6
0.3
0

Figure 7. CPT1β expression and protein oxidation in adipoVEGF-/- vs. littermate control mice. (A) Subsarcolemmal mitochondrial protein isolated from quadriceps femoris muscles of male adipoVEGF-/- (n=4) and control mice (n=4) under basal conditions probed for CPT1β, shown at 75 KDa. Ponceau S stained membrane shows equally loaded total protein in each lane. Even numbered lanes represent adipoVEGF-/- and odd numbered lanes represent control mice. (B) Quantification of CPT1β normalized to total protein. (C) Membrane showing protein oxidation using Oxyblot. Lanes 2,4,5, and 7 represent adipoVEGF-/- (n=4) and lanes 1,3, and 6 represent control mice (n=3). (D) Quantification of protein oxidation normalized to total protein. Data presented as mean ± SEM.

CHAPTER 4: SUMMARY AND DISCUSSION

The principle finding of this work is that adipose-specific VEGF deficient mice show decreased endurance running capacity without a concurrent decrease in maximal running speed. Following one hour of sub-maximal exertion, adipoVEGF-/- mice displayed decreased circulating levels of glucose, insulin, and glycerol compared to controls. These data suggest that rarefaction of adipose tissue vasculature (mediated by deficits in VEGF), and/or loss of adipose VEGF itself, blunt the availability of lipid-derived substrates from adipocyte stores during endurance exercise. This ultimately impairs endurance exercise capacity, yet decreases insulin secretion and improves insulin sensitivity.

4.1 General findings: Body and tissue mass, capillarity, and effects of age and sex

At the time of sacrifice, adipoVEGF-/- mice had half as much gonadal WAT, and one-third as much interscapular BAT (Chapter 3, Tables 1 and 2). Overall, there was a trend towards decreased percentage body fat and body mass in adipoVEGF-/- mice but these differences observed at up to 24 weeks of age were not nearly as dramatic as the difference seen in individual tissue masses and did not reach statistical significance at many time points (Chapter 3, Figure 3). The discrepancy between adipose tissue mass and body composition data could be due to the gap in age when these measurements were taken; adipose tissue masses were collected at 45 weeks old, whereas percentage body fat was collected between 6 and 24 weeks old. Unfortunately, no body composition assessment was made at the time of sacrifice. Regardless, these data are in agreement with the findings of Sung et al. (2013), that adipoVEGF-/- mice show little difference in body mass, a small decrease in body fat percentage, and dramatic decrease in gonadal fat tissue mass under basal conditions, even at younger ages (12-16 weeks). Additionally, unpublished supplementary data from our laboratory show that while high fat (HF) feeding induced increased body mass in both adipoVEGF-/- and control mice compared to their

normal chow (NC) fed counterparts (comparisons HF to NC within the same genotype group), differences in body mass with respect to *genotype* were small and did not reach statistical significance, regardless of diet (Appendix, Figure S1). However, in this same set of animals, BAT tissue mass was significantly reduced (approximately 3-fold) in both male and female adipoVEGF-/- mice compared to controls under both the HF and NC diet conditions (Appendix, Tables S1-S3). The reduction in BAT tissue mass was more dramatic under the HF condition. Overall reductions in adipoVEGF-/- WAT compared to controls under both HF and NC conditions were observed in males only, however these data were variable and not statistically significant. Notably, these animals were 19 weeks old at the time of sacrifice, but the effects seen BAT tissue mass are similar to those observed in 45-week-old mice (NC). This suggests that deficiency in adipose VEGF (affecting tissue capillarity) seems to have a more profound effect of tissue mass reduction in BAT, compared to WAT. This may also occur independently from effects of age.

Regarding the effect of age and sex in our studies, many of our experiments were conducted at an older age (approximately 40-45 weeks old). On one hand, there was the potential for effects of age to exacerbate some of our findings in already-challenged adipoVEGF-/- mice (i.e. exercise capacity, altered substrate availability and protein oxidation), however it is also possible that inevitable age-related dysfunction in both groups became a confounding factor. Regarding sex, there were no statistical differences observed in gonadal adipose tissue mass between males and females (Chapter 3, Tables 1 and 2). This could also be explained by the age of the animals at the time of sacrifice (42 weeks); although males tend to deposit more visceral fat, females experience menopause-related decreases estrogens, progestins, and androgens, which are associated with increased adipose tissue accumulation in the

abdominal region, perhaps causing them to "catch up" to males in older age (Brown *et al.*, 2010; Chen *et al.*, 2012). While males tended to have a greater body mass than females, there was no main effect for sex observed for percentage body fat between 6 and 24 weeks old.

A discrepancy also exists in our BAT findings, such that VEGF mRNA expression was decreased by 90% in adipoVEGF-/- BAT, compared to only a 50% reduction in WAT (Chapter 3, Figure 1). However, reduction in adipoVEGF-/- BAT tissue capillarity was only about 40%, similar to the reduction seen in WAT (Chapter 3, Figure 2). This suggests that there may be a compensatory mechanism acting to help maintain BAT tissue vasculature to a greater degree than in WAT. Overall, the molecular regulation of angiogenesis involves an intricate balance between positive and negative regulatory proteins (Olfert & Birot, 2011). An overall increase in BAT capillarity could be due to local upregulation of positive angiogenic factors other than VEGF (such as fibroblast growth factor and matrix metalloproteinases), acting independently from or in combination with a downregulation of anti-angiogenic factors (such as thrombospondin-1 and -2 and endostatin). BAT, as opposed to WAT, could be targeted for this compensation due to its high degree of metabolic activity and role in maintaining thermoregulation. Notably, a recent study found that BAT vascularity, specifically, plays a role in metabolism. Shimizu et al. (2014) report impaired insulin sensitivity and dysregulation of blood glucose adipoVEGF-/- mice. Associated downregulation of mitochondrial metabolic genes and increased appearance of large lipid droplets were observed in BAT, with an overall shift in BAT towards a "whitened" phenotype. With BAT-specific redelivery of VEGF, a BAT-like phenotype was recovered, along with improvements in systemic metabolic function. Capillary rarefaction also occurred in both BAT and WAT as a result of obesity and mitochondrial ROS production and instance of mitophagy markers were observed in BAT in the

obese state (Shimizu *et al.*, 2014). Overall, these findings suggest that maintenance of BAT vasculature is critical for sustaining systemic metabolic homeostasis, and point to BAT as a specific target for future investigations of the role of VEGF and adipose tissue capillarity in metabolism.

4.2 Specific aim 1

Specific Aim 1 was to determine whether decreased endurance exercise capacity in adipoVEGF-/- mice is associated with decreased FFA substrate availability during endurance exercise. It was hypothesized that adipoVEGF-/- mice would show decreased circulating FFA immediately following an exhaustive bout of endurance exercise, along with indications of greater reliance on glucose metabolism. Our preliminary findings indicated that adipoVEGF-/- mice displayed decreased endurance running capacity, without a concurrent decrease in maximal running speed (Chapter 3, Figure 4). This suggested an alteration in substrate utilization, rather than a change in maximal oxygen uptake capacity, in adipoVEGF-/- mice. In order to explain this finding, we measured circulating glucose, insulin, glycerol and FFA under basal fasted conditions, and again immediately following one hour of submaximal exercise. We found that adipoVEGF-/- mice displayed decreased circulating levels of glucose, insulin, and glycerol compared to controls following 1 hr of submaximal exertion, and that basal fasting insulin was also significantly decreased (Chapter 3, Figure 6).

Decreased circulating glycerol following submaximal exercise in adipoVEGF-/- mice suggests that glycerol and/or FFAs are not being sufficiently mobilized from adipose tissue stores for use by the working skeletal muscle during such an exercise bout. We propose that this inability to mobilize lipid-derived energy during submaximal exercise is due to decreased perfusion of the adipose tissue as a result of VEGF deficiency and the ensuing capillary

rarefaction. Alternatively, these data could also suggest a novel function for VEGF, where loss of adipocyte VEGF (via a direct mechanism) impairs the ability to move FFA into the bloodstream and/or carry FFA away from the tissue once released.

Insulin secretion is known to be blunted during prolonged low intensity exercise to allow for lipolysis (Wasserman *et al.*, 1989). This could also explain both the basal and post-exercise deficits in insulin in adipoVEGF-/- mice compared to controls. If lipid substrates are not made appropriately available at rest or during exercise, this may elicit a feedback loop to further suppress insulin secretion in attempt to bring circulating FFA to required levels. It is possible that such a compensatory mechanism may be sufficient at rest, explaining why no difference was observed in basal fasting glycerol or FFA, but insufficient under conditions of exercise-induced stress, explaining the decrease in glycerol in adipoVEGF-/- mice following exercise. Additionally, we saw no difference in glucose handling during an oral glucose tolerance test under basal conditions (Chapter 3, Figure 5). This was accompanied by a decrease in basal fasting insulin in adipoVEGF-/- mice compared to controls. Equivalent fasting blood glucose and handling of an OGTT, coupled with an overall decrease in fasting insulin suggests an increase in skeletal muscle insulin sensitivity in adipoVEGF-/- mice. Circulating blood glucose was significantly decreased in response to submaximal exercise in adipoVEGF-/- mice, however glucose uptake by skeletal muscle during exercise is not insulin dependent (Hayashi *et al.*, 1997). This suggests a reliance on glucose uptake for energy during submaximal exercise to compensate for diminished availability of lipid-derived substrates. Overall, these observations suggest that the skeletal muscles of adipoVEGF-/- mice may be adapting and becoming more insulin sensitive and efficient to make up for deficiencies in lipid substrate availability. Without such compensation, the deficit in endurance running capacity observed could have been even greater

in magnitude. Measurement of GLUT4, pyruvate, glycolytic enzymes, fatty acid translocase (CD36), CPT1β, and citrate synthase levels and/or activities immediately following endurance exercise would help to gain insight to the relative efficiency of skeletal muscle in adipoVEGF-/- mice compared to controls.

Our findings suggest that the maintenance of adipose tissue capillarity regulated by adipocyte VEGF is important in sustaining physiologic metabolic homeostasis, especially when exposed to a stressor. Studies examining the role of adipose-derived VEGF in the context of high fat feeding and obesity confirm its importance in the maintenance of overall metabolic health (Sun *et al.*, 2012; Elias *et al.*, 2012; Sung *et al.*, 2013; Shimizu *et al.*, 2014). Here, we demonstrate the consequences of submaximal exercise stress under conditions of adipose-specific VEGF deficiency, and show that the body may attempt to compensate for the loss of VEGF through decreased insulin secretion and increased skeletal muscle insulin sensitivity. This suggests a novel role for VEGF in influencing carbohydrate and lipid metabolism.

4.3 Specific aim 2

Specific Aim 2 was to determine whether adipoVEGF-/- mice exhibit decreased endurance capacity due to dysfunction induced by lipid deposition in skeletal muscle. It was hypothesized that adipoVEGF-/- mice would show increased intramuscular triglycerides and subsequent skeletal muscle dysfunction when compared to controls. To investigate this, we attempted to measure intramuscular triglycerides with oil red o staining, along with measurement of CPT1β protein expression and general protein oxidation in skeletal muscle mitochondria. Overall, no differences were observed between the groups for any of these measurements.

To rule out the possibility of adipose tissue modification leading to an unintended effect skeletal muscle capillarity, we confirmed that there was no difference in muscle capillarity in

PLT and SOL muscles (Chapter 3, Figure 2). Additionally, there was no difference in levels of VEGF mRNA expression in skeletal muscle of adipoVEGF-/- mice (Chapter 3, Figure 1), confirming the specificity of VEGF deletion to the adipose tissue.

Oil red o staining was attempted on 8μm transverse cryosections of the triceps surae muscles collected under basal conditions from these animals. However, there were several problems that occurred during this process. The quality of the cryosections was compromised such that there was folding-over of the tissue around the edges of the sections, as well as "bubbling" of the tissue in the middle of the sections; the tissue was not laying completely flat against the slide in many cases, making it difficult, if not impossible, to accurately assess muscle fat content. Moreover, after completing the oil red o staining protocol described by Goodpaster et al. (2000), accumulation of red dye and non-specific staining was observed around the edges of the muscle sections. Additionally, there were vast areas of unstained tissue in the middle of all tissue sections (Appendix, Figure S3A). These observations were not consistent with the speckling of red staining seen within the muscle fibers in example images by Goodpaster et al. (2000). As a positive control, cryosections of BAT and *db/db* soleus (SOL) muscle were stained at the same time as experimental sections (Appendix, Figure S3B). BAT staining was successful, showing consistent dark red staining within these high-lipid containing cells. The *db/db* SOL showed some positive staining, consistent with the expectation that a high intramuscular lipid content would be observed in these muscles. However, some dye clumping and non-specific staining was also observed in this control muscle tissue, again complicating the interpretation of muscle fat content. Overall, to the best of our knowledge, there was no instance of specific and/or positive oil red o staining in either adipoVEGF-/- or control samples.

However, to confirm this, the oil red o staining protocol used should be further optimized and repeated on a newly sectioned set of muscles.

Protein expression of CPT1β in subsarcolemmal mitochondria isolated from quadriceps femoris muscles was measured (Chapter 3, Figure 7) in attempt to gauge differences in fatty acid oxidation between the groups, which may have been associated with differences endurance exercise capacity. A change in CPT1β expression could have several implications. First, as mentioned in regards to specific aim 1, upregulation or downregulation of CPT1β could simply correlate to magnitude of fatty acid oxidation affected by FFA made available to the muscles. However, regarding specific aim 2, there are two theories surrounding lipid-induced skeletal muscle damage and levels of β-oxidation. First, it is contended that decreased β–oxidation causes accumulation of lipids and hinders insulin signaling (Yu *et al.*, 2002). On the other hand, there is evidence that excessive β–oxidation overloads mitochondrial metabolic capacity and leads to incomplete fatty acid oxidation and an accumulation of metabolic intermediates, causing mitochondrial stress, protein oxidation, and decrease in function (Koves *et al.*, 2008). In our mouse model, no differences were observed in CPT1β protein expression in adipoVEGF-/- mice compared to controls. To further investigate the current findings, CPT1β could be measured in younger animals, from tissue extracted immediately following exercise, and/or in samples from the more oxidative soleus muscle. The intermyofibrillar population could also be included in the mitochondrial extraction protocol to achieve a more complete analysis.

General protein oxidation was also measured to investigate oxidative damage within the muscles of adipoVEGF-/- mice (Figure 6). The fact that no difference was observed between the two groups of mice suggests that loss of adipocyte VEGF may not influence oxidative stress. However, these experiments should also be repeated using mitochondria isolated from the more

oxidative soleus muscle, including the intermyofibrillar population. Samples from younger animals could also be examined, as protein oxidation due to older age could have been a confounding variable in this experiment.

Overall, based on our present findings, it seems unlikely that the difference observed in endurance running capacity can be attributed directly to increased intramuscular lipid content or mitochondrial dysfunction.

4.4 Additional future work and concerns

It will be important to expand the current findings in order to gain a more specific and quantitative understanding of FFA release into circulation directly from the adipose tissue and lipid uptake by working skeletal muscle. Quantification of HSL phosphorylation in adipose tissue under basal fasted conditions would aid in addressing this. Additionally, adipose triglyceride lipase (ATGL) could be measured. ATGL is a recently characterized protein with triglyceride-specific lipase activity, is regulated by insulin, and thought to be an important contributor to adipocyte lipolysis (Kershaw *et al.*, 2006). Levels of CD36 expression could also be quantified to assess transport of FFA into the muscle cells and mitochondria. Examining muscle glycogen content, as FFA availability is known to affect glycogen depletion, could also provide important information (Costill *et al.*, 1977). Availability of glycerol and FFA affected by adipose tissue vascularity may impact muscle glycogen synthesis and/or glycogen depletion during exercise in this model.

Regarding exercise protocols, additional work to support the findings of this study need to include measurement of RER during the entire duration of a prolonged bout of endurance running. Additionally, conducting endurance testing using swimming instead of treadmill running might help to achieve a more stringent "forced exercise" protocol without dependence

on the use of electrical shock. A concern associated with treadmill running is that determination of the point of exhaustion for each animal can become subjective when some animals exhibit better running behavior that others. In some cases, an animal will become conditioned to avoid the electric shock at the end of the belt (by positioning the exposed skin of their feet between the bars the shock grid such that the metal only touches their fur and they don't feel the shock) and may refuse to run despite not having reached a state of complete exhaustion. With a swimming protocol, the innate fear of drowning should allow for better determination of when true exhaustion occurs and therefore differences in exercise capacity may be more accurately observed.

It could be valuable to repeat the present experiments using a mouse model possessing a different promoter to drive adipose-specific VEGF deletion. With a 50% decrease in VEGF mRNA expression in WAT, and concurrent 40% decrease in capillarity in WAT in our adipoVEGF-/- model, it is possible that our findings, especially those pertaining to post-exercise circulating glycerol and FFA could be exacerbated and gain higher statistical significance in a model with a greater knockdown efficiency and consequently a more dramatic reduction in adipose tissue vascularization. It has been indicated that the adiponectin promoter may be more efficient for this type of model (Lee *et al.*, 2013).

Finally, concerns have been raised regarding the running speeds used during submaximal endurance testing and the 1 hr run prior to serum sampling and how these speeds correlate with oxygen uptake and reliance on fat usage during these exercise bouts. As stated in the Methods section of Chapter 3, based on previously published data, running speed correlates closely with oxygen uptake in untrained mice and rats, and maximal treadmill running speed ranges between 35 and 45 m/min in untrained C57BL/6 mice (Høydal *et al.*, 2007; Olfert *et al.*, 2009; Malek &

Olfert, 2009). Based on these data and a running speed of 20 m/min, the percent effort at which endurance running tests were conducted ranged from 44% to 57%, and should not have exceeded 43% of maximal running speed for the 1-hour run prior to serum sampling (conducted at 15 m/min).

Maximal running speed testing was completed specifically in the experimental adipoVEGF-/- and littermate control mice at two age points (25 and 37 weeks) following the last endurance running test. No difference was observed in maximal running speed, confirming that percent effort should have been similar between the groups at the same running speed during the endurance tests. Additionally, we are also able to compare complied unpublished data on maximal running speeds attained from over 100 mice from various lines at various ages to create a linear regression (Appendix, Figure S2A) that allows us to estimate maximal running speed at a given age (speed attained declines with age). Based on these data, our mice completed the fist endurance run test at approximately 50% effort (6 weeks old). Percent effort only reached about 57% with increasing age by 24 weeks old (Appendix, Figure S2B). These estimations are consistent with the estimation based on the published work of Høydal et al. (2007) and Malek & Olfert (2009). The "crossover concept" describes a shift from reliance on fat to carbohydrate metabolism with increasing exercise intensity. Exercising at approximately 40% aerobic power elicits about 50% reliance on fat usage, while 60% aerobic power correlates with about 40% reliance on fat usage (Brooks & Mercier, 1994). Since our animals generally did not exceed 57% effort during endurance runs in this study, we believe our mice were exercising at an intensity correlating with greater reliance on fat as an energy substrate. While it would be ideal to actually measure oxygen uptake during each endurance test, the use of maximal running speed has been shown to be a good surrogate that correlates with VO2 max in rodents.

4.5 Translational Significance

Better understanding the purpose of adipose VEGF in exercise will lead to an increased overall understanding of its physiological function. This understanding will be important in developing effective therapeutic manipulations of the VEGF pathway in conjunction with exercise-based therapies. Elevated circulating levels of VEGF have been shown in obese individuals and studies have investigated the prospect of inhibiting VEGF action in adipose tissue as a means of adipocyte ablation to treat obesity (Kolonin *et al.*, 2004; Cao, 2010; Wada *et al.*, 2011). However, this notion is countered by recent evidence from Sung et al. (2013) and Shimizu et al. (2014), which emphasizes the importance of maintained adipose tissue capillarity in sustaining overall metabolic health, and our data, which further suggest a role in maintenance of appropriate substrate availability during submaximal exertion. Furthermore, the condition of adipose tissue in adipoVEGF-/- mice is similar to what is observed in human adipose tissue during obesity, such that it is undervascularized, hypoxic and inflammatory (Sun *et al.*, 2011; Sung *et al.*, 2013). Therefore, the notion that reductions in adipose capillarity can affect substrate availability during submaximal exercise could be applied to diet and exercise prescription targeted at the treatment of obesity. This could also influence considerations for anti-VEGF therapies along with diet and exercise prescription in cancer patients and survivors. Finally, indications of improved skeletal muscle efficiency and insulin sensitivity in adipoVEGF-/- mice were observed in our experiments, possibly as a compensatory mechanism for deficits in availability of lipid derived substrates. If these findings are confirmed, they may provide headway for the manipulation of the VEGF protein and/or pathway in the development of treatments to combat diabetes.

4.6 Conclusion

In conclusion, adipose VEGF is an important regulator of adipose tissue vascularity, which is essential for proper metabolic function during prolonged, submaximal exercise conditions. In agreement with our first hypothesis (specific aim 1) adipose VEGF plays an important role in the availability of lipid-derived substrate availability during endurance exercise. In contrast with our second hypothesis, (specific aim 2) it does not appear that this deprivation of adipose-specific VEGF leads to direct evidence of skeletal muscle dysfunction. However, we cannot exclude the possibility that adaptations *improving* skeletal muscle efficiency may also be occurring in order to compensate for the deficiency caused by a decrease in lipid-derived substrate availability.

REFERENCES

Baynard T, Vieira-Potter VJ, Valentine RJ & Woods J a (2012). Exercise training effects on inflammatory gene expression in white adipose tissue of young mice. *Mediators Inflamm* **2012,** 767953.

Björntorp P, Bergman H & Varnauskas E (1969). Plasma free fatty acid turnover rate in obesity. *Acta Med Scand* **185,** 351–356.

Bloch-Damti A & Bashan N (2005). Proposed mechanisms for the induction of insulin resistance by oxidative stress. *Antioxid Redox Signal* **7,** 1553–1567.

Bonen A, Luiken JJ, Arumugam Y, Glatz JF & Tandon NN (2000). Acute regulation of fatty acid uptake involves the cellular redistribution of fatty acid translocase. *J Biol Chem* **275,** 14501–14508.

Bonner JS, Lantier L, Hasenour CM, James FD, Bracy DP & Wasserman DH (2013). Muscle-specific vascular endothelial growth factor deletion induces muscle capillary rarefaction creating muscle insulin resistance. *Diabetes* **62,** 572–580.

Brooks GA & Mercier J (1994). Balance of carbohydrate and lipid utilization during exercise: the "crossover" concept. *J Appl Physiol* **76,** 2253–2261.

Brown LM, Gent L, Davis K & Clegg DJ (2010). Metabolic impact of sex hormones on obesity. *Brain Res* **1350,** 77–85.

Byrne AM, Bouchier-Hayes DJ & Harmey JH (2005). Angiogenic and cell survival functions of vascular endothelial growth factor (VEGF). *J Cell Mol Med* **9,** 777–794.

Cao Y (2010). Adipose tissue angiogenesis as a therapeutic target for obesity and metabolic diseases. *Nat Rev Drug Discov* **9,** 107–115.

Chen X, McClusky R, Chen J, Beaven SW, Tontonoz P, Arnold AP & Reue K (2012). The number of x chromosomes causes sex differences in adiposity in mice. *PLoS Genet* **8,** e1002709.

Cooke JP (2002). Nitric Oxide and Angiogenesis. *Circulation* **105,** 2133–2135.

Costill DL, Coyle E, Dalsky G, Evans W, Fink W & Hoopes D (1977). Effects of elevated plasma FFA and insulin on muscle glycogen usage during exercise. *J Appl Physiol* **43,** 695–699.

Elias I, Franckhauser S, Ferré T, Vilà L, Tafuro S, Muñoz S, Roca C, Ramos D, Pujol A, Riu E, Ruberte J & Bosch F (2012). Adipose tissue overexpression of vascular endothelial growth factor protects against diet-induced obesity and insulin resistance. *Diabetes* **61,** 1801–1813.

Fontana L & Klein S (2007). Aging, adiposity, and calorie restriction. *JAMA* **297,** 986–994.

Fulton D, Gratton JP, McCabe TJ, Fontana J, Fujio Y, Walsh K, Franke TF, Papapetropoulos A & Sessa WC (1999). Regulation of endothelium-derived nitric oxide production by the protein kinase Akt. *Nature* **399,** 597–601.

Gerber HP, Hillan KJ, Ryan AM, Kowalski J, Keller GA, Rangell L, Wright BD, Radtke F, Aguet M & Ferrara N (1999). VEGF is required for growth and survival in neonatal mice. *Development* **126,** 1149–1159.

Gille H, Kowalski J, Li B, LeCouter J, Moffat B, Zioncheck TF, Pelletier N & Ferrara N (2001). Analysis of biological effects and signaling properties of Flt-1 (VEGFR-1) and KDR (VEGFR-2). A reassessment using novel receptor-specific vascular endothelial growth factor mutants. *J Biol Chem* **276,** 3222–3230.

Goodpaster BH, Theriault R, Watkins SC & Kelley DE (2000). Intramuscular lipid content is increased in obesity and decreased by weight loss. *Metabolism* **49,** 467–472.

Gorman JL, Liu STK, Slopack D, Shariati K, Hasanee A, Olenich S, Olfert IM & Haas TL (2014). Angiotensin II evokes angiogenic signals within skeletal muscle through co-ordinated effects on skeletal myocytes and endothelial cells. *PLoS One* **9,** e85537.

Hatano D, Ogasawara J, Endoh S, Sakurai T, Nomura S, Kizaki T, Ohno H, Komabayashi T & Izawa T (2011). Effect of exercise training on the density of endothelial cells in the white adipose tissue of rats. *Scand J Med Sci Sports* **21,** e115–21.

Hayashi T, Wojtaszewski JF & Goodyear LJ (1997). Exercise regulation of glucose transport in skeletal muscle. *Am J Physiol* **273,** E1039–51.

He W, Barak Y, Hevener A, Olson P, Liao D, Le J, Nelson M, Ong E, Olefsky JM & Evans RM (2003). Adipose-specific peroxisome proliferator-activated receptor gamma knockout causes insulin resistance in fat and liver but not in muscle. *Proc Natl Acad Sci U S A* **100,** 15712–15717.

Hoeben ANN, Landuyt B, Highley MS, Wildiers H, Oosterom ATVAN & Bruijn EADE (2004). Vascular Endothelial Growth Factor and Angiogenesis. *Pharmacol Rev* **56,** 549–580.

Horowitz JF (2003). Fatty acid mobilization from adipose tissue during exercise. *Trends Endocrinol Metab* **14,** 386–392.

Høydal MA, Wisløff U, Kemi OJ & Ellingsen O (2007). Running speed and maximal oxygen uptake in rats and mice: practical implications for exercise training. *Eur J Cardiovasc Prev Rehabil* **14,** 753–760.

Hultman E (1973). Energy metabolism in human muscle. *J Physiol* **231,** 56P.

Iyer N V, Kotch LE, Agani F, Leung SW, Laughner E, Wenger RH, Gassmann M, Gearhart JD, Lawler AM, Yu AY & Semenza GL (1998). Cellular and developmental control of O2 homeostasis by hypoxia-inducible factor 1 alpha. *Genes Dev* **12,** 149–162.

Kershaw EE, Hamm JK, Verhagen LAW, Peroni O, Katic M & Flier JS (2006). Adipose triglyceride lipase: function, regulation by insulin, and comparison with adiponutrin. *Diabetes* **55,** 148–157.

Khaidakov M, Heflich RH, Manjanatha MG, Myers MB & Aidoo A (2003). Accumulation of point mutations in mitochondrial DNA of aging mice. *Mutat Res* **526,** 1–7.

Kolonin MG, Saha PK, Chan L, Pasqualini R & Arap W (2004). Reversal of obesity by targeted ablation of adipose tissue. *Nat Med* **10,** 625–632.

Koves TR, Ussher JR, Noland RC, Slentz D, Mosedale M, Ilkayeva O, Bain J, Stevens R, Dyck JRB, Newgard CB, Lopaschuk GD & Muoio DM (2008). Mitochondrial overload and incomplete fatty acid oxidation contribute to skeletal muscle insulin resistance. *Cell Metab* **7,** 45–56.

Lee KY, Russell SJ, Ussar S, Boucher J, Vernochet C, Mori M a, Smyth G, Rourk M, Cederquist C, Rosen ED, Kahn BB & Kahn CR (2013). Lessons on conditional gene targeting in mouse adipose tissue. *Diabetes* **62,** 864–874.

Leung DW, Cachianes G, Kuang WJ, Goeddel D V & Ferrara N (1989). Vascular endothelial growth factor is a secreted angiogenic mitogen. *Science* **246,** 1306–1309.

Maglione D, Guerriero V, Viglietto G, Delli-Bovi P & Persico MG (1991). Isolation of a human placenta cDNA coding for a protein related to the vascular permeability factor. *Proc Natl Acad Sci U S A* **88,** 9267–9271.

Malek MH & Olfert IM (2009). Global deletion of thrombospondin-1 increases cardiac and skeletal muscle capillarity and exercise capacity in mice. *Exp Physiol* **94,** 749–760.

Nagy a (2000). Cre recombinase: the universal reagent for genome tailoring. *Genesis* **26,** 99–109.

Neufeld G, Cohen T, Gengrinovitch S & Poltorak Z (1999). Vascular endothelial growth factor (VEGF) and its receptors. *FASEB J* **13,** 9–22.

Olenich SA, Audet GN, Szeszel-Federowicz V, Chen D & Olfert IM (2012). Novel functional relationships between VEGF and energy metabolism identified by microarray analysis. *Exp Biol*.

Olfert IM & Birot O (2011). Importance of anti-angiogenic factors in the regulation of skeletal muscle angiogenesis. *Microcirculation* **18,** 316–330.

Olfert IM, Howlett RA, Tang K, Dalton ND, Gu Y, Peterson KL, Wagner PD & Breen EC (2009). Muscle-specific VEGF deficiency greatly reduces exercise endurance in mice. *J Physiol* **587,** 1755–1767.

Olfert IM, Howlett R a, Wagner PD & Breen EC (2010). Myocyte vascular endothelial growth factor is required for exercise-induced skeletal muscle angiogenesis. *Am J Physiol Regul Integr Comp Physiol* **299,** R1059–67.

Park JE, Chen HH, Winer J, Houck KA & Ferrara N (1994). Placenta growth factor. Potentiation of vascular endothelial growth factor bioactivity, in vitro and in vivo, and high affinity binding to Flt-1 but not to Flk-1/KDR. *J Biol Chem* **269,** 25646–25654.

Park JE, Keller GA & Ferrara N (1993). The vascular endothelial growth factor (VEGF) isoforms: differential deposition into the subepithelial extracellular matrix and bioactivity of extracellular matrix-bound VEGF. *Mol Biol Cell* **4,** 1317–1326.

Pascual M, Larralde J & Martínez JA (1995). Insulin-like growth factor I (IGF-I) affects plasma lipid profile and inhibits the lipolytic action of growth hormone (GH) in isolated adipocytes. *Life Sci* **57,** 1213–1218.

Powers SK & Howley ET (2007). *Exercise Physiology: Theory and Application to Fitness and Performance*, 6th edn.ed. Barrosse E. McGraw-Hill Companies, New York.

Safdar A, Bourgeois JM, Ogborn DI, Little JP, Hettinga BP, Akhtar M, Thompson JE, Melov S, Mocellin NJ, Kujoth GC, Prolla TA & Tarnopolsky MA (2011). Endurance exercise rescues progeroid aging and induces systemic mitochondrial rejuvenation in mtDNA mutator mice. *Proc Natl Acad Sci U S A* **108,** 4135–4140.

Samuel VT, Petersen KF & Shulman GI (2010). Lipid-induced insulin resistance: unravelling the mechanism. *Lancet* **375,** 2267–2277.

Schreurs M, Kuipers F & van der Leij FR (2010). Regulatory enzymes of mitochondrial beta-oxidation as targets for treatment of the metabolic syndrome. *Obes Rev* **11,** 380–388.

Shimizu I, Aprahamian T, Kikuchi R, Shimizu A, Papanicolaou KN, MacLauchlan S, Maruyama S & Walsh K (2014). Vascular rarefaction mediates whitening of brown fat in obesity. *J Clin Invest* **124,** 2099–2112.

Sun K, Kusminski CM & Scherer PE (2011). Adipose tissue remodeling and obesity. *J Clin Invest* **121,** 2094–2101.

Sun K, Wernstedt I, Kusminski CM, Carolina A, Wang Z V, Pollard JW, Brekken RA & Scherer PE (2012). Dichotomous effects of VEGF-A on adipose tissue dysfunction. *Proc Natl Acad Sci* **109,** 5874–5879.

Sung H-K, Doh K-O, Son JE, Park JG, Bae Y, Choi S, Nelson SML, Cowling R, Nagy K, Michael IP, Koh GY, Adamson SL, Pawson T & Nagy A (2013). Adipose vascular endothelial growth factor regulates metabolic homeostasis through angiogenesis. *Cell Metab* **17,** 61–72.

Surwit RS, Kuhn CM, Cochrane C, McCubbin JA & Feinglos MN (1988). Diet-induced type II diabetes in C57BL/6J mice. *Diabetes* **37,** 1163–1167.

Terman BI, Carrion ME, Kovacs E, Rasmussen BA, Eddy RL & Shows TB (1991). Identification of a new endothelial cell growth factor receptor tyrosine kinase. *Oncogene* **6,** 1677–1683.

Wada H, Ura S, Kitaoka S, Satoh-Asahara N, Horie T, Ono K, Takaya T, Takanabe-Mori R, Akao M, Abe M, Morimoto T, Murayama T, Yokode M, Fujita M, Shimatsu A & Hasegawa K (2011). Distinct characteristics of circulating vascular endothelial growth factor-a and C levels in human subjects. *PLoS One* **6,** e29351.

Waki H & Tontonoz P (2007). Endocrine functions of adipose tissue. *Annu Rev Pathol* **2,** 31–56.

Wasserman DH, Lacy DB, Goldstein RE, Williams PE & Cherrington AD (1989). Exercise-induced fall in insulin and increase in fat metabolism during prolonged muscular work. *Diabetes* **38,** 484–490.

Weisberg SP, McCann D, Desai M, Rosenbaum M, Leibel RL & Ferrante AW (2003). Obesity is associated with macrophage accumulation in adipose tissue. *J Clin Invest* **112,** 1796–1808.

Yach D, Stuckler D & Brownell KD (2006). Epidemiologic and economic consequences of the global epidemics of obesity and diabetes. *Nat Med* **12,** 62–66.

Yokota T, Kinugawa S, Hirabayashi K, Matsushima S, Inoue N, Ohta Y, Hamaguchi S, Sobirin MA, Ono T, Suga T, Kuroda S, Tanaka S, Terasaki F, Okita K & Tsutsui H (2009). Oxidative stress in skeletal muscle impairs mitochondrial respiration and limits exercise capacity in type 2 diabetic mice. *Am J Physiol Heart Circ Physiol* **297,** H1069–77.

Yu C, Chen Y, Cline GW, Zhang D, Zong H, Wang Y, Bergeron R, Kim JK, Cushman SW, Cooney GJ, Atcheson B, White MF, Kraegen EW & Shulman GI (2002). Mechanism by which fatty acids inhibit insulin activation of insulin receptor substrate-1 (IRS-1)-associated phosphatidylinositol 3-kinase activity in muscle. *J Biol Chem* **277,** 50230–50236.

APPENDIX

Table S1. Body and tissue masses- male and female mice at 19 wks old (mean±SEM)

	High Fat		Normal Chow		Main Effect p Value			
	adipoVEGF-/-	Control	adipoVEGF-/-	Control	Genotype	Diet	Sex	Interaction
	n=14	n=25	n=12	n=17				
Body mass (g)	23.6±1.2	26.6±1.4#	22.7±1.7	21.4±0.9	n.s.	<0.01	<0.0001	n.s.
Heart mass (mg)	99.0±2.3	106.8±2.9	97.3±4.9	98.9±2.2	n.s.	n.s.	<0.0001	n.s.
Heart mass/body mass (mg/g)	4.3±0.1	4.1±0.1#	4.4±0.2	4.7±0.1	n.s.	<0.01	<0.0001	n.s.
Lung mass (mg)	182.0±5.7	183.7±3.5#	176.3±9.3	167.5±3.4	n.s.	<0.05	<0.01	n.s.
Kidney mass (mg)	159.8±5.9	159.0±6.6#	147.5±7.5	136.5±5.0	n.s.	<0.01	<0.0001	n.s.
WAT mass (mg)	602.1±120.5	960.2±140.7#	384.5±81.8	375.3±69.9	n.s.	<0.001	<0.0001	<0.01 (Diet*Sex)
BAT mass (mg)	49.3±6.1†	163.4±18.2	51.3±6.2§	112.1±14.3	<0.0001	n.s.	<0.001	<0.05 (Genotype*Sex)
Gastrocnemius mass (mg)	152.3±6.4	139.9±3.9	137.7±8.6	134.3±4.5	n.s.	p=0.51	<0.05	n.s.

Main effect p values for 2-way ANOVA. †p<0.05 comparing adipoVEGF-/- to littermate controls within the high fat (HF) group, §p<0.05 comparing adipoVEGF-/- to littermate controls within the normal chow (NC) group. #p<0.05 comparing HF to NC within the littermate control group.

Table S2. Body and tissue masses- male mice at 19 wks old (mean±SEM)

	High Fat		Normal Chow		Main Effect p Value		
	adipoVEGF-/-	Control	adipoVEGF-/-	Control	Genotype	Diet	Genotype*Diet
	n=6	n=15	n=7	n=8			
Body mass (g)	26.7±2.3	30.1±1.6	26.0±2.1	24.4±1.1	n.s.	n.s.	n.s.
Heart mass (mg)	103.9±3.3	112.8±3.9	105.7±6.0	104.0±2.3	n.s.	n.s.	n.s.
Heart mass/body mass (mg/g)	4.0±0.2	3.8±0.1#	4.1±0.1	4.3±0.2	n.s.	<0.05	n.s.
Lung mass (mg)	189.2±10.6	188.0±5.4	192.6±12.1	169.9±4.9	n.s.	n.s.	n.s.
Kidney mass (mg)	171.4±11.1	179.6±7.1#	160.2±10.4	151.4±5.4	n.s.	<0.05	n.s.
WAT mass (mg)	966.3±155.7*	1386.5±139.0#	523.7±113.9	613.6±103.6	n.s.	<0.001	n.s.
BAT mass (mg)	68.7±8.0†	206.2±24.3	56.9±8.8§	149.2±26.4	<0.0001	n.s.	n.s.
Gastrocnemius mass (mg)	155.5±10.0	142.8±5.9	150.6±6.4	138.0±6.7	n.s.	n.s.	n.s.

Main effect p values for 2-way ANOVA. †p<0.05 comparing adipoVEGF-/- to littermate controls within the high fat (HF) group, §p<0.05 comparing adipoVEGF-/- to littermate controls within the normal chow (NC) group. *p<0.05 comparing HF to NC within the adipoVEGF-/- group, #p<0.05 comparing HF to NC within the littermate control group.

Table S3. Body and tissue masses- female mice at 19 wks old (mean±SEM)

	High Fat		Normal Chow		Main Effect p Value		
	adipoVEGF-/-	Control	adipoVEGF-/-	Control	Genotype	Diet	Genotype*Diet
	n=8	n=10	n=5	n=9			
Body mass (g)	21.2±0.4*	21.3±1.3	18.2±0.7	18.8±0.5	n.s.	<0.01	n.s.
Heart mass (mg)	95.4±2.8	97.9±2.5	85.6±4.9	94.3±2.9	n.s.	<0.05	n.s.
Heart mass/body mass (mg/g)	4.5±0.1	4.6±0.1	4.7±0.3	5.0±0.1	n.s.	n.s.	n.s.
Lung mass (mg)	176.7±5.8*	177.8±3.8	153.5±5.9	165.4±4.9	n.s.	<0.01	n.s.
Kidney mass (mg)	151.1±4.7*†	132.3±4.0	129.8±3.0	124.9±5.4	<0.05	<0.01	n.s.
WAT mass (mg)	290.0±38.4	320.7±119.0	189.6±26.1	190.0±15.2	n.s.	n.s.	n.s.
BAT mass (mg)	34.8±4.1†	99.2±8.2	41.5±5.4§	83.2±6.1	<0.0001	n.s.	n.s.
Gastrocnemius mass (mg)	149.9±8.8	135.5±4.9	119.8±16.3	131.1±6.3	n.s.	<0.05	n.s.

Main effect p values for 2-way ANOVA. †p<0.05 comparing adipoVEGF-/- to littermate controls within the high fat (HF) group, §p<0.05 comparing adipoVEGF-/- to littermate controls within the normal chow (NC) group. *p<0.05 comparing HF to NC within the adipoVEGF-/- group.

A

	High Fat		Normal Chow	
	adipoVEGF-/-	Control	adipoVEGF-/-	Control
Males and Females	n=14	n=25	n=12	n=17
Males	n=6	n=15	n=7	n=8
Females	n=8	n=10	n=5	n=9

B

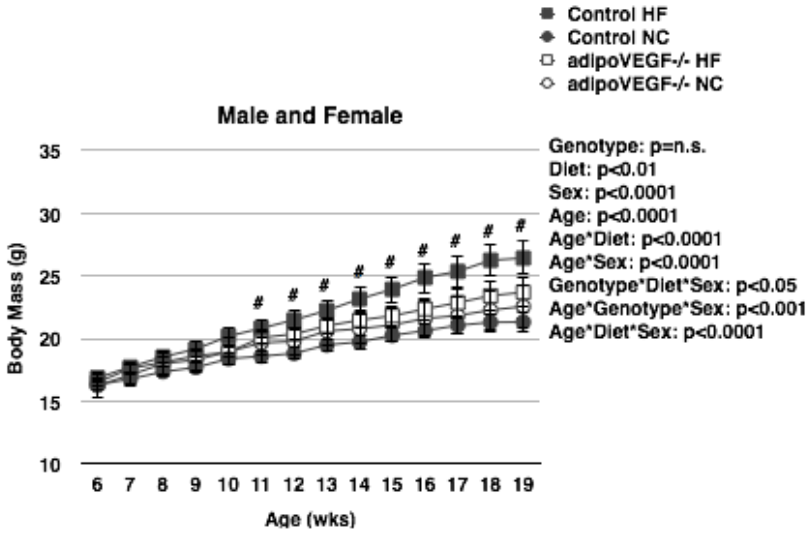

C

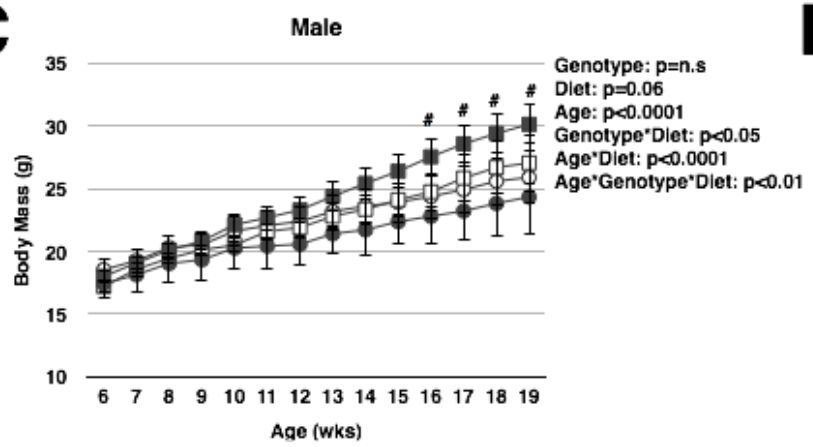

D

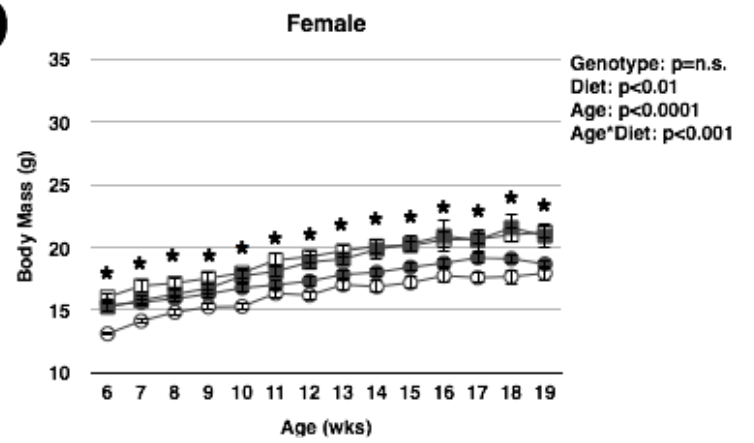

Figure S1. Body mass of adipoVEGF-/- vs. littermate control mice on a high fat and normal chow diet. Breakdown (A) of n per group by diet, genotype, and sex. Body mass (B-D) on a high fat (HF) or normal chow (NC) diet between 6 and 19 wks old in adipoVEGF-/- and littermate control mice. Data presented as mean±SEM. Main effect values reported using repeated measures ANOVA. *$p<0.05$ comparing HF to NC within the adipoVEGF-/- group, #$p<0.05$ comparing HF to NC within the littermate control group.

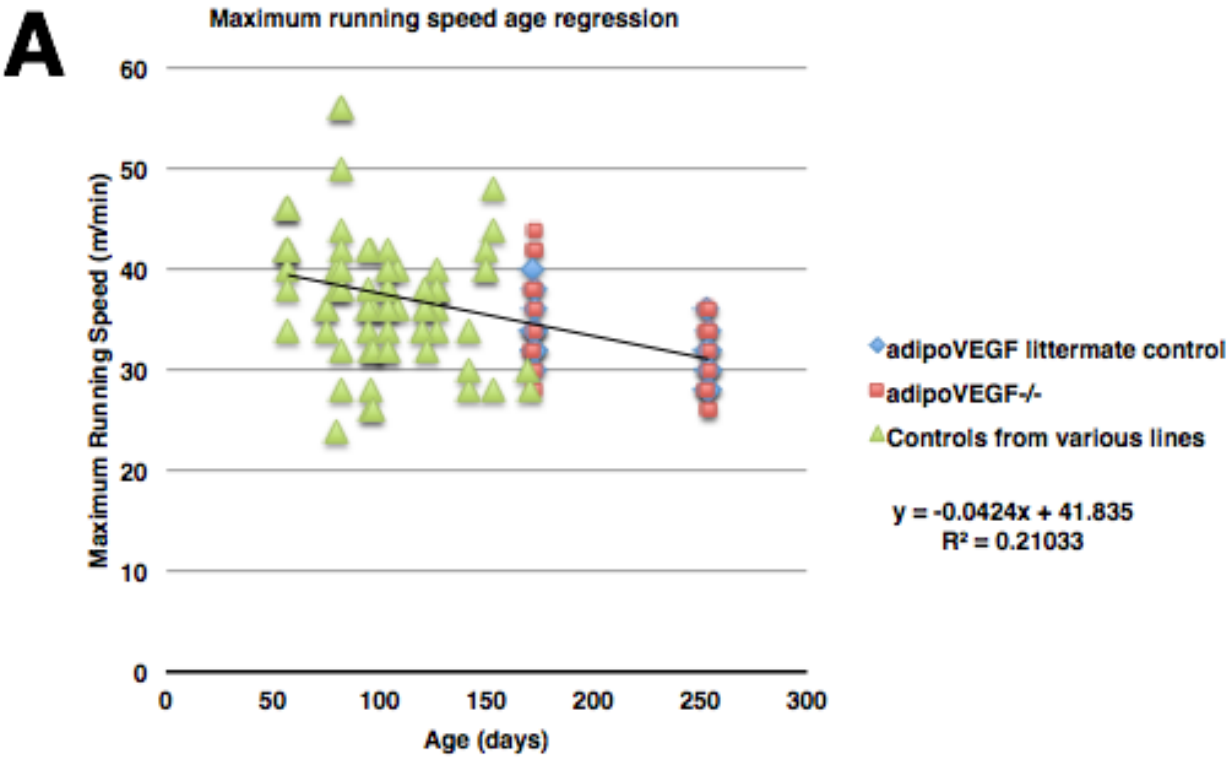
A
Maximum running speed age regression
Maximum Running Speed (m/min)
60
50
40
30
20
10
0
0
50
100
150
200
250
300
Age (days)
adipoVEGF littermate control
adipoVEGF-/-
Controls from various lines
y = -0.0424x + 41.835
R² = 0.21033

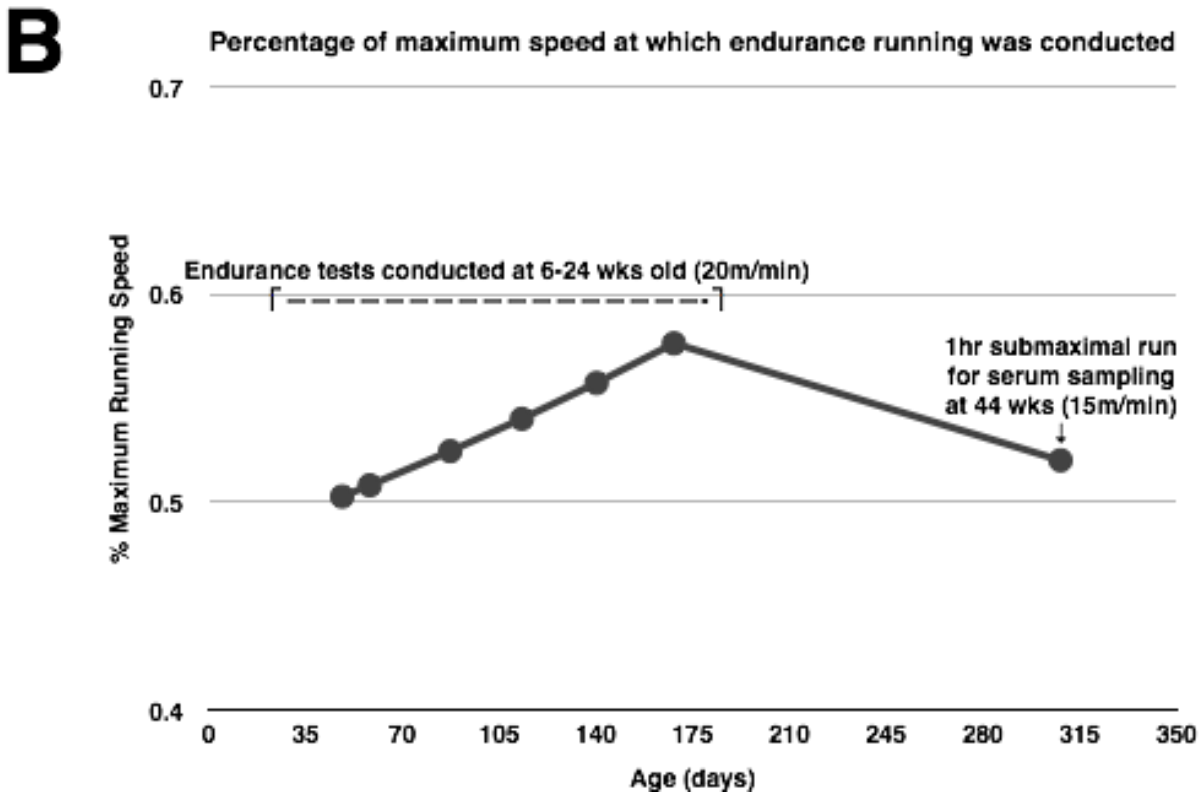
B
Percentage of maximum speed at which endurance running was conducted
0.7
Endurance tests conducted at 6-24 wks old (20m/min)
0.6
1hr submaximal run
for serum sampling
at 44 wks (15m/min)
% Maximum Running Speed
0.5
0.4
0
35
70
105
140
175
210
245
280
315
350
Age (days)

Figure S2. Use of predicted maximal running speed to determine submaximal effort for endurance testing in adipoVEGF-/- and littermate control mice. (A) Maximal running speed achieved at various ages in various lines of mice. Linear regression represents the age-associated rate of decline in performance. (B) The linear regression shown in panel A was used to extrapolate an estimated maximal running speed for all mice (adipoVEGF-/- and littermate controls treated equally) for each age at which endurance running testing was conducted. The estimated maximal running speed correlating with a given age was used to calculate the percentage maximal running speed at which the endurance test was conducted, based on the speed used for that test (20m/min for tests between 6 and 24 wks and 15 m/min for 1hr run at 44 wks old).

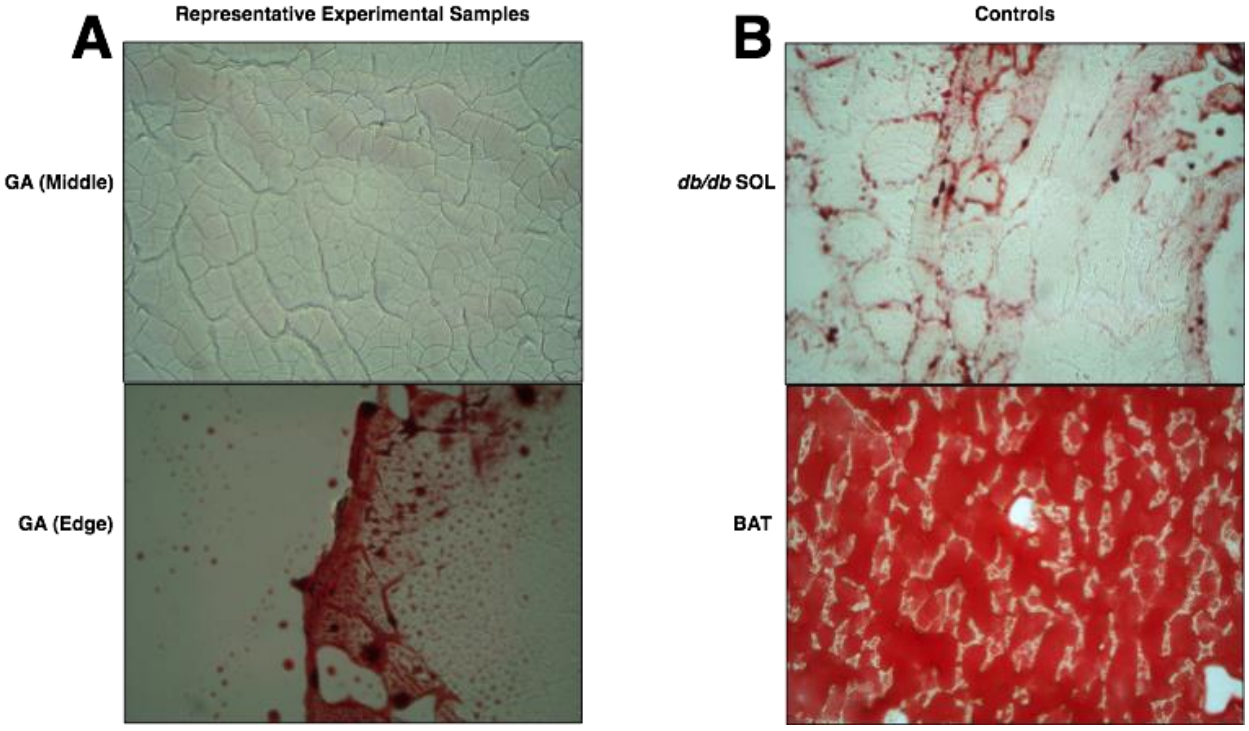
A
Representative Experimental Samples
GA (Middle)
GA (Edge)
B
Controls
db/db SOL
BAT

Figure S3. Attempted oil red o staining in experimental and control tissues. (A) Representative images of oil red o staining attempted on gastrocnemius muscle (GA) cryosections from experimental animals. Absence of staining in the middle, and clumped dye with non-specific staining around edges was consistently seen in both adipoVEGF-/- and littermate control tissues. Muscles were collected under basal conditions at 45 weeks old. (B) Staining on control tissue cryosections including *db/db* soleus muscle (SOL) and brown adipose tissue (BAT). BAT staining was successful; SOL staining also showed some specificity, but dye clumping and non-specific staining also occurred.